

Original Research

Deciphering a Prognostic Signature Based on Soluble Mediators Defines the Immune Landscape and Predicts Prognosis in HNSCC

Hao Chi^{1,2,†}, Gaoge Peng^{2,†}, Guobin Song³, Jinhao Zhang³, Xixi Xie², Jinyan Yang², Jiayu Xu⁴, Jieying Zhang⁵, Ke Xu^{6,*}, Qibiao Wu^{1,*}, Guanhu Yang^{7,*}¹Faculty of Chinese Medicine, Macau University of Science and Technology, 999078 Taipa, Macau, China²Clinical Medical College, Southwest Medical University, 646000 Luzhou, Sichuan, China³School of Stomatology, Southwest Medical University, 646000 Luzhou, Sichuan, China⁴School of Science, Minzu University of China, 100081 Beijing, China⁵First Teaching Hospital of Tianjin University of Traditional Chinese Medicine, 300072 Tianjin, China⁶Department of Oncology, Chongqing General Hospital, 401147 Chongqing, China⁷Department of Specialty Medicine, Ohio University, Athens, OH 45701, USA*Correspondence: nsmcxuke@163.com (Ke Xu); qbwu@must.edu.mo (Qibiao Wu); guanhuayang@gmail.com (Guanhu Yang)

†These authors contributed equally.

Academic Editor: Sukmook Lee

Submitted: 7 October 2023 Revised: 29 November 2023 Accepted: 8 January 2024 Published: 22 March 2024

Abstract

Background: The study on Head and Neck Squamous Cell Carcinoma (HNSCC), a prevalent and aggressive form of head and neck cancer, focuses on the often-overlooked role of soluble mediators. The objective is to leverage a transcriptome-based risk analysis utilizing soluble mediator-related genes (SMRGs) to provide novel insights into prognosis and immunotherapy efficacy in HNSCC patients. **Methods:** We analyzed the expression and prognostic significance of 10,859 SMRGs using 502 HNSCC and 44 normal samples from the TCGA-HNSC cohort in The Cancer Genome Atlas (TCGA). The samples were divided into training and test sets in a 7:3 ratio, with an additional external validation using 40 tumor samples from the International Cancer Genome Consortium (ICGC). Key differentially expressed genes (DEGs) with prognostic significance were identified through univariate and Lasso-Cox regression analyses. A prognostic model based on 20 SMRGs was developed using Lasso and multivariate Cox regression. We assessed the clinical outcomes and immune status in high-risk (HR) and low-risk (LR) HNSCC patients utilizing the BEST databases and single-sample Gene Set Enrichment Analysis (ssGSEA). **Results:** The 20 SMRGs were crucial in predicting the prognosis of HNSCC, with the SMRG signature emerging as an independent prognostic indicator. Patients classified in the HR group exhibited poorer outcomes compared to those in the LR group. A nomogram, integrating clinical characteristics and risk scores, demonstrated substantial prognostic value. Immunotherapy appeared to be more effective in the LR group, possibly attributed to enhanced immune infiltration and expression of immune checkpoints. **Conclusions:** The model based on soluble mediator-associated genes offers a fresh perspective for assessing the pre-immune efficacy and showcases robust predictive capabilities. This innovative approach holds significant promise in advancing the field of precision immuno-oncology research, providing valuable insights for personalized treatment strategies in HNSCC.

Keywords: soluble mediators; HNSCC; tumor microenvironment; immunotherapy; nomogram; prognostic signature

1. Introduction

Head and neck squamous cell carcinoma (HNSCC), a critical global health concern, ranks as the sixth most prevalent cancer worldwide. This group of malignancies, originating in the oral cavity, lips, nasopharynx, pharynx, and larynx, presents a significant clinical challenge [1,2]. Annually, HNSCC accounts for more than 809,000 new cases and over 316,000 deaths, constituting approximately 3.6% of all cancer-related fatalities [3]. The prognosis for HNSCC remains daunting despite the array of available therapeutic interventions, including surgery, chemotherapy, radiotherapy, and photodynamic therapy. The increasing morbidity and mortality rates each year underscore the urgent need for enhanced treatment strategies, as the cancer's aggressive and heterogeneous nature complicates manage-

ment and therapeutic outcomes [4]. Early-stage HNSCC patients have a 60–95% success rate with primary tumor resection and neck debulking [5], but most are diagnosed at advanced stages with metastasis and recurrence [6,7]. Disease prognosis heavily depends on the Tumour, node and metastasis (TNM) stage and histologic grade, influencing treatment decisions, including immunotherapy [8]. However, traditional clinicopathological staging may not accurately reflect prognosis due to variable clinicopathologic characteristics in patients with the same clinical stage [9].

Soluble mediators like cytokines, chemokines, and growth factors play pivotal roles in the tumor microenvironment (TME), influencing immune responses and intercellular communication [10,11]. These mediators facilitate tumor growth, chronic inflammation, and an immunosuppressive and pro-angiogenic milieu, challenging the effi-



cacy of therapies including immunotherapy [12]. Tumor-associated macrophages, for instance, release soluble mediators (e.g., IL-6, IL-10, CCL18, CCL22, TNF α , TGF- β) promoting tumor signaling [13–19]. The immunosuppressive TME in HNSCC is further exacerbated by various soluble mediators [20], with some (TGF- β , VEGF, IL-10) known to dampen immune responses [21]. Recent studies highlight the prognostic potential of soluble mediators in various cancers [22–24], with markers like soluble mannose receptors (sMRs) and soluble hemoglobin scavenger receptors (sCD163) relevant in gastric cancer prognosis [25], and soluble CD155 predicting liver cancer survival.

Amidst evolving bioinformatics, this study, for the first time, explores the prognostic and therapeutic implications of soluble mediator-related genes (SMRGs) in HNSCC using the Cancer Genome Atlas-Head and Neck Squamous Cell Carcinoma (TCGA-HNSC) dataset. We meticulously analyzed the association between SMRG expression patterns and HNSCC prognosis, identifying 20 reliable SMRGs. This investigation was driven by the unexplored potential of SMRGs in diagnosing and prognosticating HNSCC. Consequently, we developed a predictive model based on SMRGs and a risk score, examining their ties to the immune microenvironment, and associations with chemotherapy and immunotherapy. This comprehensive genetic analysis aims to underscore the utility of SMRGs in enhancing prognosis, diagnosis, and personalized treatment strategies for HNSCC patients.

2. Method

2.1 Data Sources

The TCGA-HNSC cohort, encompassing 502 HNSC and 44 normal samples, was retrieved from the TCGA database (<https://portal.gdc.cancer.gov/>), with 501 HNSC samples possessing complete clinical data included in subsequent analyses. These samples were randomized into training and test risk groups (7:3 ratio) using the *caret* R package (<https://cran.r-project.org/web/packages/caret/index.html>), drawing on relevant clinical information. Additionally, 40 patients with comprehensive follow-up data were sourced from the ICGC as an external validation set.

2.2 Difference Analysis and Enrichment Analysis

Differential expression analysis between normal and tumor groups was meticulously executed using the ‘*limma*’ R package [26–28], adhering to stringent criteria of an absolute log fold change ($|\log_{2}FC|$) greater than 1 and an adjusted *p*-value threshold below 0.05. This approach facilitated the identification of genes significantly altered in HNSCC compared to normal tissue. Further, we employed the ‘*clusterProfiler*’ R package (version 4.1.3) [29,30] to conduct comprehensive enrichment analysis of Gene Ontology (GO) and Kyoto Encyclopedia of Genes and Genomes (KEGG) pathways, setting a significance threshold at a *p*-value of less than 0.05. The GO enrichment analysis delved into the

molecular functions (MF), biological processes (BP), and cellular components (CC) associated with these differentially expressed genes. Concurrently, the KEGG pathway analysis provided insights into the biological pathways implicated in HNSCC, thereby enhancing our understanding of the molecular underpinnings of this complex disease.

2.3 Consensus Clustering Analysis

TCGA-HNSC cohorts were segregated into distinct groups based on the consensus expression of soluble mediator-associated differentially expressed genes (DE-SMRGs) using ‘*ConsensusClusterPlus*’ R software (Version 4.1.3, Chapel Hill, NC, USA) [31]. The *MCPcounter* R package (Version 4.1.3, Paris, France) [32] was employed to evaluate the content of immune-related cells in these clusters and to generate violin plots.

2.4 Model Construction and Validation

The prognostic value of SMRGs in the HNSCC cohort was meticulously evaluated through univariate Cox regression analysis. This statistical approach allowed us to determine the individual impact of each SMRG on patient survival. Further, to refine our analysis and identify the most influential genes within the vast array of SMRGs, we employed LASSO Cox regression analysis using the ‘*glmnet*’ R package [33]. This method effectively pinpointed key genes and their corresponding regression coefficients, reducing the risk of overfitting by penalizing the complexity of the model. The risk scores for each patient were then calculated using a comprehensive formula that combines the expression levels of these key mRNAs and their respective regression coefficients. The formula is structured as follows: $\text{risk score} = \text{Expression_mRNA1} \times \text{Coef_mRNA1} + \text{Expression_mRNA2} \times \text{Coef_mRNA2} + \dots + \text{Expression_mRNAn} \times \text{Coef_mRNAn}$. This risk scoring system encapsulates the cumulative impact of multiple gene expressions on the prognosis of HNSCC, enabling a more nuanced and precise prediction of clinical outcomes.

2.5 Model Formulae

Risk scores for patients in our study were accurately computed using the ‘*survminer*’ R package, based on the established model equations derived from the combination of gene expressions and their corresponding coefficients. This calculation enabled the categorization of patients into high-risk (HR) and low-risk (LR) groups, a division based on the median value of the calculated risk scores. Following this stratification, survival curves for each group were meticulously plotted to visually represent and compare the survival probabilities over time between these two distinct risk categories. To quantitatively assess the predictive accuracy of our prognostic model, the concordance index (C-index) was determined using the ‘*pec*’ R program. The C-index is a crucial metric in survival analysis, providing a measure of the model’s ability to accurately predict sur-

vival outcomes [34]. Additionally, we utilized the ‘survivalROC’ R package for conducting time-dependent Receiver Operating Characteristic (ROC) curve analysis. This analysis is essential for evaluating the predictive potential of the genetic markers identified in our study over time, offering insights into the temporal robustness and reliability of the prognostic model in assessing patient outcomes in HNSCC.

2.6 Independent Prognostic Analysis and Nomogram Construction

The evaluation of the risk score’s effectiveness as an independent prognostic factor for HNSCC was thoroughly conducted using both univariate and multivariate Cox regression models. These models are instrumental in discerning the extent to which the calculated risk score can predict patient outcomes independently of other clinical variables. Furthermore, to translate our findings into a practical tool for clinical use, we utilized the “rms” R package [35] to create detailed nomograms. These nomograms integrate several key parameters, including the risk score derived from our model, patient age, tumor stage, and the expression levels of the model genes. They are designed to predict the 1, 3, and 5-year overall survival rates for patients in the TCGA HNSC cohort.

2.7 Immunity Analysis of the Risk Signature

We employed a multifaceted approach to quantify immune infiltration scores, utilizing a suite of established methodologies. These included XCELL [36,37], TIMER [38,39], QUANTISEQ [40,41], MCPCOUNT [32], EPIC [42], CIBERSORT [43,44] and CIBERSORT-ABS [45]. The integration of these diverse tools enabled a thorough analysis of the immune landscape within the HNSCC tumor microenvironment. We conducted Spearman correlation analysis to investigate the relationship between the calculated risk scores and the presence of various immune cells, providing insights into the interplay between genetic risk factors and the immune milieu. Furthermore, the single-sample Gene Set Enrichment Analysis (ssGSEA) method was applied to determine the immune cell characteristics in HNSCC patients. This approach was instrumental in differentiating the immune infiltration status between high-risk (HR) and low-risk (LR) groups, offering a nuanced understanding of how risk levels correlate with immune response.

Our analysis extended to examining 20 suppressive immune checkpoints identified in Auslander’s study [46], focusing on their variations between the HR and LR groups. Additionally, we referenced a gene set pertaining to the cancer immune cycle from Xu *et al.*’s website [44] (<http://biocc.hrbmu.edu.cn/TIP/>) and drew upon Mariathasan’s research for a list of genes associated with favorable responses to the anti-PD-L1 drug atezolizumab [47]. To assess the enrichment of gene features related to the cancer immune cycle and immunotherapy response, we employed

the Gene Set Variation Analysis (GSVA) method [48] was employed. A p -value of less than 0.05 was considered indicative of a significant difference between the HR and LR groups. The ‘ggcor’ R package (version 4.1.3) was utilized to further analyze the association between risk scores and these genetic characteristics, providing a comprehensive overview of how genetic risk factors might influence the efficacy of immunotherapeutic interventions in HNSCC.

2.8 Drug Sensitivity

The evaluation of treatment response in high-risk (HR) and low-risk (LR) patient groups with HNSCC was meticulously conducted using half-maximal inhibitory concentration (IC50) data. This data was sourced from the Genomics of Drug Sensitivity in Cancer (GDSC) database, accessible at <https://www.cancerrxgene.org/>. Utilizing the “pRRophetic” R package (version 4.1.3) [49], we were able to predict and compare the response of HR and LR groups to various anticancer drugs.

2.9 Tumor Immune Single Cell Hub Database

The Tumor Immune Single-Cell Hub (TISCH) database, accessible at <http://tisch.comp-genomics.org>, played a pivotal role in our research, particularly in the study of tumor microenvironment (TME) heterogeneity in HNSCC. As a comprehensive repository of single-cell RNA sequencing data, TISCH specializes in providing detailed insights into the TME across a variety of cancer types, datasets, and cell types [50].

2.10 Immunohistochemical Analysis

The verification of the expression levels of soluble mediator-related genes (SMGs) in our study on HNSCC was significantly bolstered by utilizing immunohistochemical sections from the Human Protein Atlas (HPA) database (<https://www.proteinatlas.org/>). HPA is an extensive resource that integrates proteomic, transcriptomic, and systems biology data to provide a comprehensive view of human protein expression across various tissues and cells.

2.11 Statistical Analysis

In our comprehensive study, all statistical analyses were rigorously performed using R software, version 4.1.3. We adhered to stringent statistical criteria, considering both p -values and false discovery rate (FDR) q -values below the threshold of 0.05 to denote statistical significance. This approach ensured a robust and reliable interpretation of our data, minimizing the likelihood of false positives and providing a solid foundation for our conclusions.

3. Result

3.1 Soluble Mediators Related Genes are Associated with Immunological Function

The graphic flowchart in Fig. 1 succinctly encapsulates the methodology and structure of our extensive study

on the role of SMRGs in HNSCC. Our research entailed a detailed analysis of clinical information and mRNA expression data from 546 HNSCC samples, which were sourced from The Cancer Genome Atlas (TCGA). In the initial phase of our study, we identified a comprehensive gene set of soluble mediators, totaling 10,859 genes, from the Genecard database. This extensive list served as a foundational reference for our subsequent analyses. Employing the “limma” R package, we conducted differential gene expression analysis on HNSCC tumor tissues. We set a stringent threshold of an absolute \log_2 fold change ($|\log_2FC|$) greater than 1, which led to the identification of 1943 upregulated and 537 downregulated genes (Fig. 2A). To visually represent these findings, a heatmap was generated, showcasing the mRNA expression differences between tumor samples ($n = 502$) and normal samples ($n = 44$) (Fig. 2B). This visualization provided an immediate and clear comparison of gene expression patterns between the two sample types. Further, we intersected the differentially expressed genes identified in tumor samples with the initial soluble mediator gene set. This intersection resulted in the identification of 2361 differentially expressed SMRGs (DE-SMRGs). These DE-SMRGs were then subjected to further analysis using the ClusterProfiler R package for Gene Ontology (GO) and Kyoto Encyclopedia of Genes and Genomes (KEGG) enrichment. The criteria for significant enrichment were set at an adjusted p -value (p_{adj}) of less than 0.05 and a false discovery rate (FDR) of less than 0.25. The results of this enrichment analysis were presented in bubble maps (Fig. 2C,D), highlighting the top 25 GO and top 20 KEGG enrichment results. These results predominantly showed enrichment in pathways related to T cell activation, lymphocyte regulation, and immune responses, including Th1 and Th2 cell differentiation, T cell receptor signaling, TNF signaling, and IL-17 signaling pathways. The enrichment in these specific pathways underscores the potential immunological functions and implications of SMRGs in the pathology of HNSCC.

3.2 Immunological Clustering of DE-SMRGs in Two Clusters with Different Clinical Outcomes of HNSCC

We categorized the TCGA-HNSC cohort into groups based on expression of DE-SMRGs using the ConsensusClusterPlus R program (Supplementary Figs. 1,2). A consensus matrix with k value equal to 2 was found to minimize crossover between HNSC samples (Fig. 3A). Survival differences between clusters were analyzed using the ClusterSurvival R package, revealing better overall survival (OS) in one cluster compared to the other (Fig. 3B). To elucidate the reasons behind these prognostic differences, we examined the levels of immune-related cells in both clusters using the MCPcounter R package, including B lineage, CD8 T cells, cytotoxic lymphocytes, endothelial cells, monocyte lineage, bone marrow dendritic cells, NK cells, and T cells. We found significantly higher infiltration of these cells in

one cluster (Fig. 3C–J), suggesting a correlation between immune cell infiltration and better patient prognosis in HNSCC.

3.3 Construction and Validation of SMRGs Signature and Its Prognostic Value

In our study, we developed a sophisticated risk score model based on SMRGs to predict outcomes in HNSCC patients. Initially, univariate Cox analysis, executed via the “survival” R package, identified 274 prognostic-related SMRGs ($p < 0.05$). Further refinement through lasso regression analysis distilled these to 45 key SMRGs (Fig. 4A,B, Supplementary Table 1). Employing a multifactorial Cox proportional hazard regression model, we narrowed down to 20 pivotal SMRGs, specifically *CSF2*, *ITGA4*, *LGALS3BP*, *EPO*, *EZH2*, *SFRP1*, *PSMA1*, *TNFRSF4*, *GRIA3*, *CYP2D6*, *SLC25A4*, *CCNA1*, *PRPS1*, *UCN2*, *CCL28*, *HEXA*, *SPINK1*, *HTN3*, *TLL1*, and *SPINK6* (Fig. 4C). The corresponding regression coefficients for these genes were calculated as follows: 0.3415, -0.5791, 0.9097, -0.7959, -0.5625, -0.1741, 0.8485, -0.8744, -0.8864, -0.7582, 0.5207, 0.3389, 1.4621, -0.3439, -0.3837, 1.2022, 0.4666, 0.484, 0.4744, and -0.3499. This linear prediction model, derived from multivariate Cox analysis, based on 20 weighted SMRGs, allowed us to calculate a patient-specific risk score.

To ensure the robustness of our prognostic model, we divided the patients into a training cohort ($n = 353$) and a testing cohort ($n = 148$), following a 7:3 ratio. The training cohort results aligned with the overall findings, where HR patients had significantly worse outcomes ($p < 0.001$) (Fig. 4D), and the ROC curve area under the curve (AUC) values for 1, 3, and 5-year predictions were 0.745, 0.838, and 0.839, respectively (Fig. 4G). This trend was consistent in the testing cohort, with HR patients demonstrating poorer prognoses ($p = 0.017$) (Fig. 4E), although the ROC curve AUCs at 1, 3, and 5 years were 0.708, 0.635, and 0.564, respectively (Fig. 4H). For external validation, we utilized 40 samples from the International Cancer Genome Consortium (ICGC) database as an independent test cohort. The results were consistent with the earlier findings, indicating a poorer prognosis for HR patients ($p = 0.022$) (Fig. 4F), and the ROC curves showed AUCs of 0.850 at 1 year and 0.870 at 1.5 years (Fig. 4I).

To explore the biological mechanisms behind the aberrant expression of the 20 target genes, we conducted gene correlation analysis (Fig. 4J) and pathway analysis. The pathway analysis revealed significant involvement of these SMRGs in regulating critical processes such as apoptosis, epithelial-mesenchymal transition (EMT), DNA damage response, and the cell cycle, among other tumor-related pathways (Fig. 4K). We further classified these pathways into activated (A) and repressed (I) categories, as depicted in Fig. 4L. Notably, these genes were found to influence the activation of the PI3K/AKT pathway in HNSCC pa-

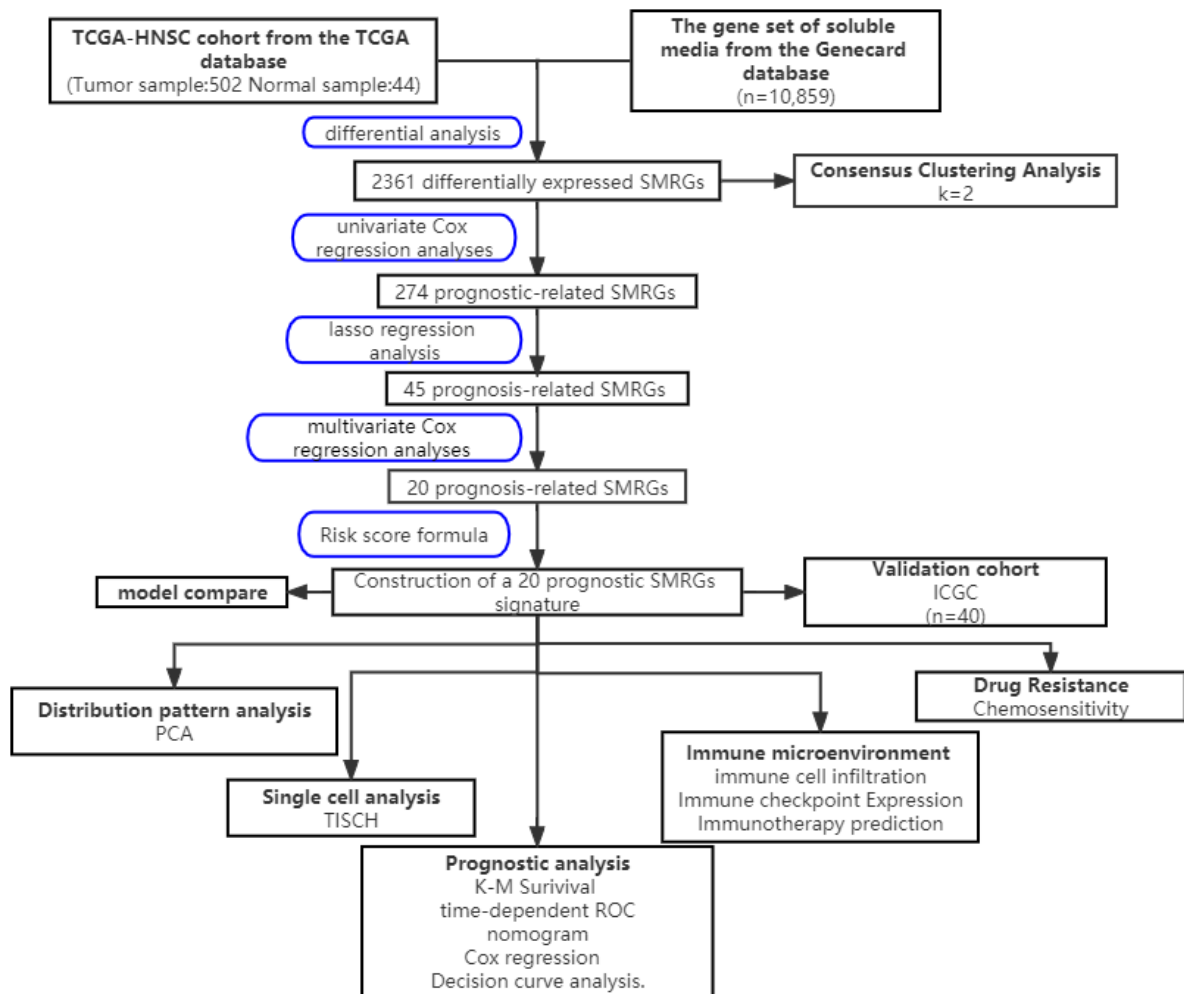


Fig. 1. The workflow of identification of the SMRGs signature for patients with HNSCC. PCA, principal components analysis; TCGA, The Cancer Genome Atlas; SMRGs, soluble mediator-related genes; ICGC, International Cancer Genome Consortium; TISCH, Tumor Immune Single-Cell Hub; ROC, Receiver Operating Characteristic; HNSCC, Head and Neck Squamous Cell Carcinoma; K-M, Kaplan-Meier.

tients. Other pathways, including apoptosis, EMT, RTK, RAS/MAPK, cell cycle, Hormone ER, Hormone AR, and DNA damage response, exhibited varying degrees of activation or repression.

3.4 Clinical Subgroup Analysis of the SMRGs Risk Model

We undertook a detailed clinical subgroup analysis to evaluate the variations in patient prognosis across diverse clinical parameters. This analysis was essential to understand how different patient characteristics might influence outcomes when assessed through the lens of our SMRGs risk model. To this end, we meticulously stratified the HNSCC patient cohort into various subgroups. These subgroups were based on critical clinical criteria such as T stage (T1-2 and T3-4), pathological stage (I-III and III-IV), pathological N stage (grades N0 and N1-3), tumor grade (grades I-II and III-IV), age (≥ 65 years), and gender (male

and female), as illustrated in Fig. 5. The stratification allowed us to conduct a nuanced and comprehensive analysis of survival outcomes across these different subgroups. Remarkably, the results consistently indicated that patients in the high-risk (HR) group, as determined by our SMRGs risk model, had significantly poorer overall survival (OS) in all the clinical subgroups examined (Fig. 5). This finding not only validates the predictive strength of our risk model but also highlights its applicability and robustness across various clinical scenarios in HNSCC. It underscores the potential of the SMRGs-based risk model as a powerful prognostic tool capable of guiding treatment decisions and predicting outcomes in a wide range of clinical contexts within HNSCC management.

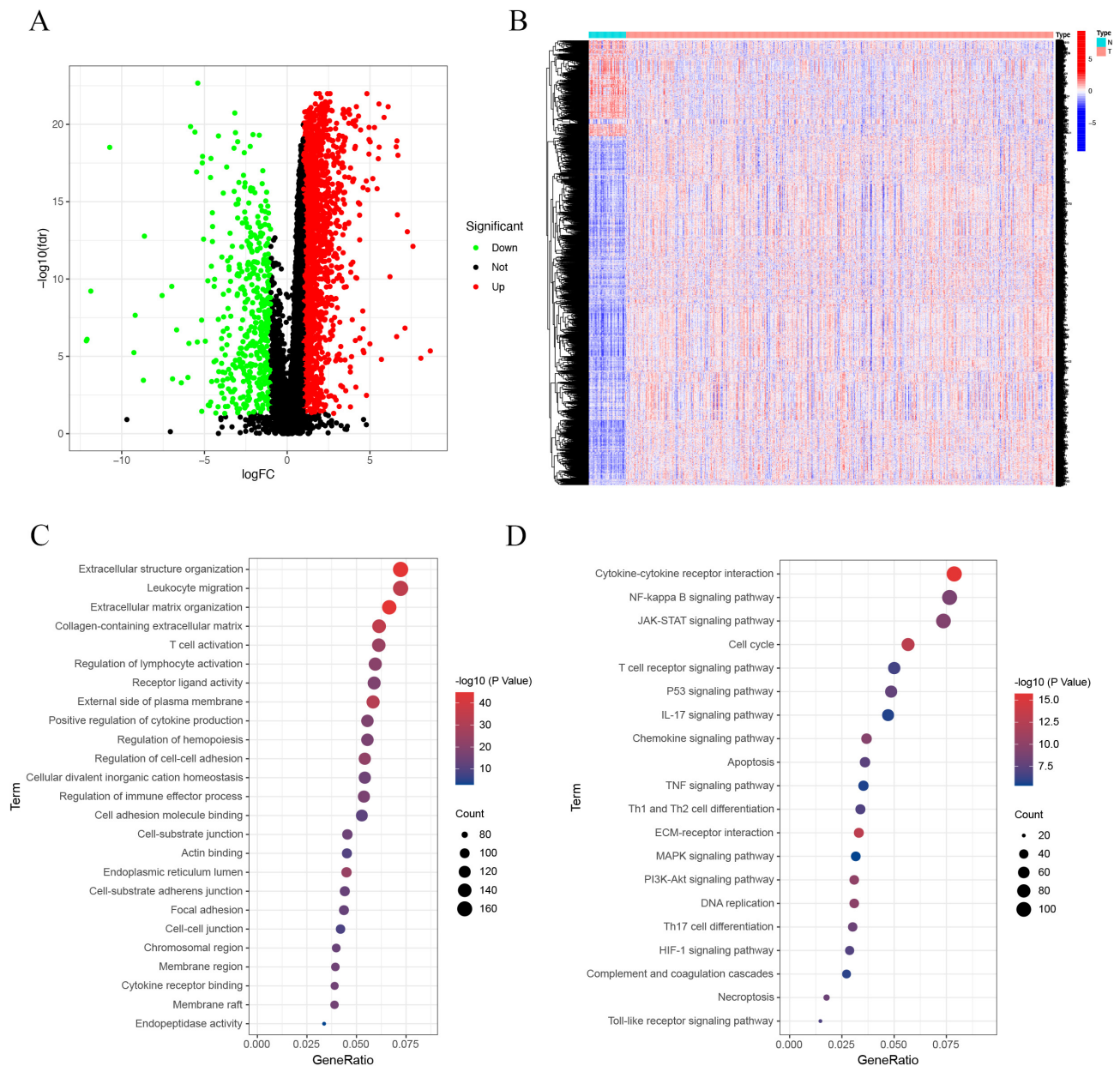


Fig. 2. Biological process analysis of soluble mediators related genes. (A) Volcano map of DE-SMRGs. (B) DE-SMRGs in HNSCC tumor samples and normal samples. (C) GO enrichment analysis DE-SMRGs. (D) KEGG pathway analysis of DE-SMRGs. DE-SMRGs, differentially expressed SMRGs; GO, Gene Ontology; KEGG, Kyoto Encyclopedia of Genes and Genomes; FC, fold change.

3.5 Nomogram Construction in Conjunction with Clinical Features

Our in-depth study on HNSCC entailed rigorous univariate and multivariate Cox regression analyses to evaluate the prognostic potential of our SMRGs-based model. These analyses were crucial for determining whether our 20-SMRGs-based prognosis signature could act as an independent prognostic factor, considering the overall survival (OS) of HNSCC patients in conjunction with their clinical characteristics. The univariate analysis yielded significant findings, revealing a strong correlation between several clinical parameters—age, stage, grade, T, N—and the

risk score with patient prognosis ($p < 0.001$) (Fig. 6A). This association underscored the relevance of these clinical factors in determining patient outcomes. Moving to the multivariate analysis, the risk score continued to stand out as a robust and independent prognostic indicator within our patient cohort ($p < 0.01$) (Fig. 6B). To further illustrate these relationships, a heatmap was generated, showcasing the association between the expression levels of the 20 identified SMRGs in our prognostic risk model and various clinical parameters—age, grade, stage, T, N, and risk score—across all HNSCC patient samples from the TCGA (Fig. 6C). In an effort to enhance the clinical utility of our risk model, we

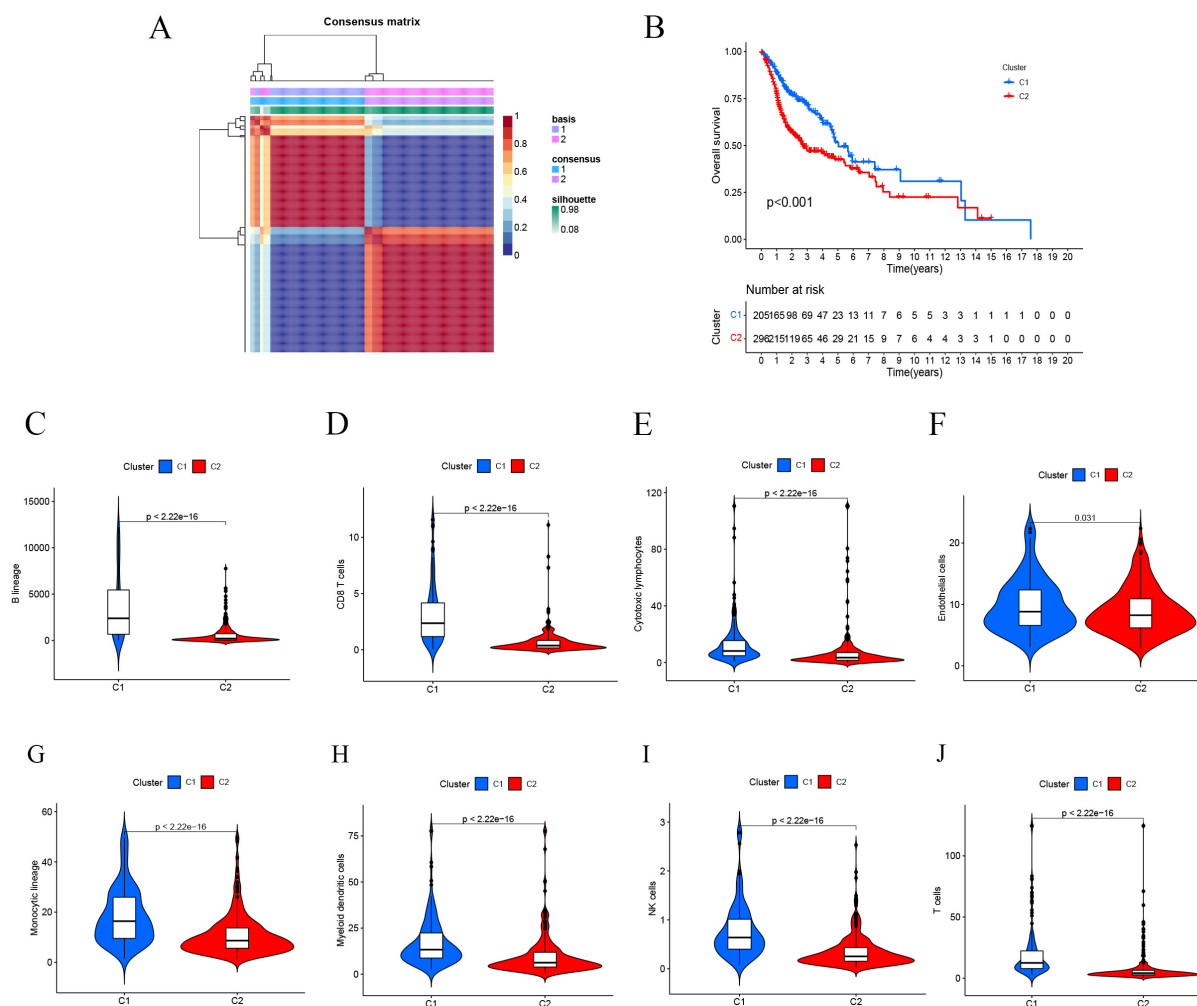


Fig. 3. Immunotyping of differentially expressed genes associated with soluble mediators. (A) Consensus clustering matrix for $K = 2$. **(B)** Survival curves of different immune genotypes. **(C–J)** The content of important immune cells among different types.

developed a comprehensive nomogram. This nomogram incorporated a range of variables: age, grade, stage, T, N, the expression levels of the 20 SMRGs, and the risk score, to predict 1, 3, and 5-year survival probabilities for HNSCC patients (Fig. 6D). The results from the nomogram clearly highlighted the dominance of the risk score in predicting OS, suggesting that our 20-SMRGs-based model offers a more precise prognostic prediction for HNSCC compared to conventional clinical parameters. The accuracy and reliability of this nomogram were further validated through calibration curves, which showed a close match between the predicted and observed values for 1-year, 3-year, and 5-year OS (Fig. 6E). Notably, the AUC value of 0.731 for the risk score derived from the 20 SMRGs demonstrated its superior predictive power for HNSCC prognosis, surpassing that of common clinicopathological features such as age, grade, pathological stage, T, and N (Fig. 6F). This finding reinforces the model's significance in clinical decision-making, evidenced by its high net benefit depicted in the decision curve analysis (Fig. 6G).

3.6 In Prognostic Prediction, the SMRGs Signature Outperformed Others

We developed a novel SMRGs signature and compared its predictive power against four established HNSCC prognostic signatures: the Lian signature [51], Tang signature [52], Xue signature [53], and Huang signature [54] (Fig. 7A–D). Uniform risk scores were calculated for each HNSCC sample across all TCGA cohorts to ensure a standardized comparison. Time-dependent ROC curve analysis revealed that our SMRGs signature consistently outperformed the other signatures, exhibiting higher AUC values at 1-year, 3-year, and 5-year survival intervals. Notably, it achieved the highest C-index of 0.718 (Fig. 7E), demonstrating superior predictive performance. This underscores the potential of our SMRGs signature as a more effective prognostic tool in HNSCC, offering enhanced accuracy in predicting patient outcomes and informing personalized treatment strategies.

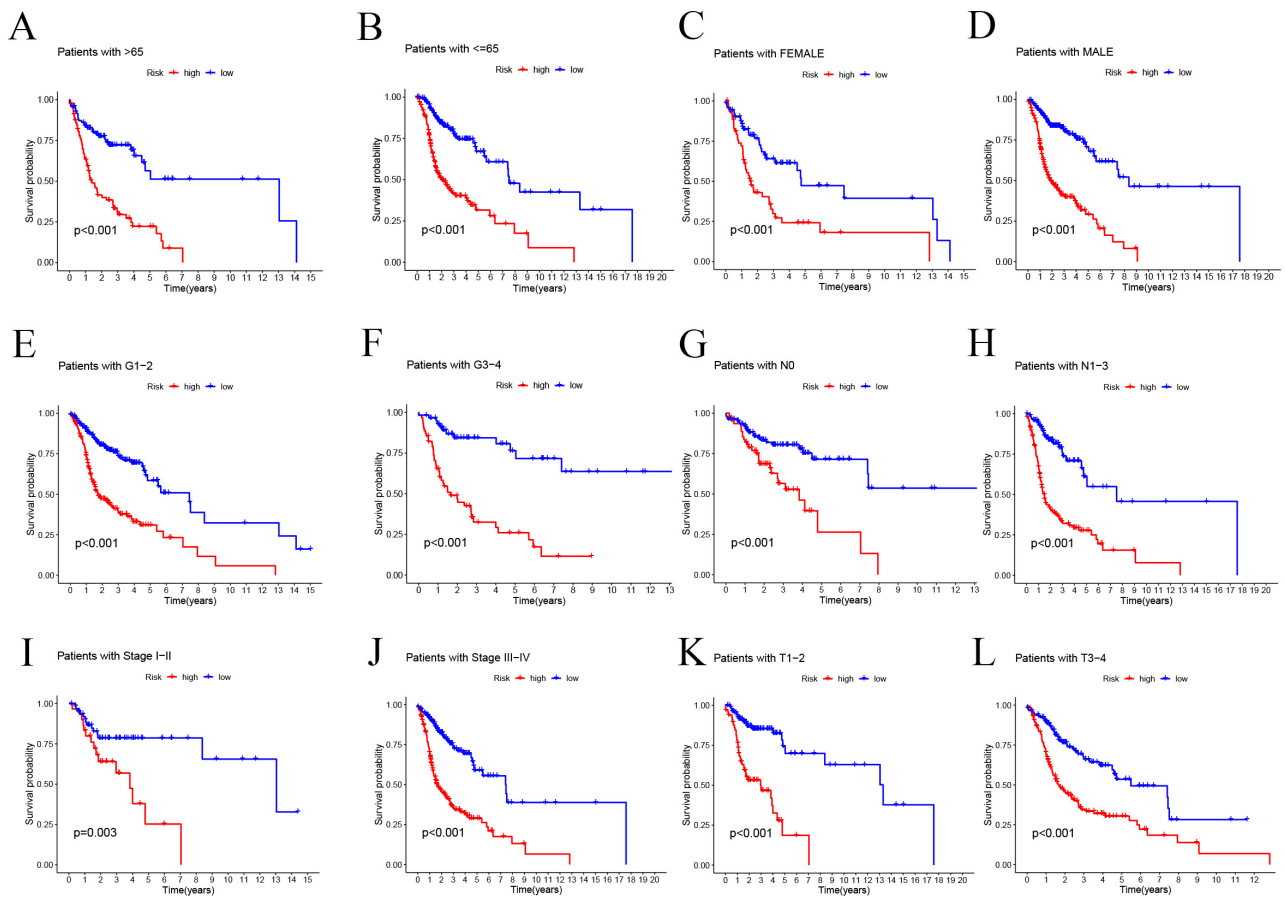


Fig. 5. Prognostic power of the SMRGs risk model for overall survival for multiple HNSC subtypes. (A) Age >65 years. (B) Age ≤65 years. (C) Female. (D) Male. (E) Grade 1–2. (F) Grade 3–4. (G) N0. (H) N1–3. (I) Stage I–II. (J) Stage III–IV. (K) T1–2. (L) T3–4.

3.7 Correlation Analysis of Risk Scores and Clinicopathological Characteristics

We explored the correlation between our SMRGs-based risk models and key clinicopathological characteristics of patients. Using the Wilcoxon test, we analyzed variations in risk scores across subgroups defined by gender, T stage, pathological stage, tumor grade, and age. The results indicated no significant association between risk scores and age, N stage, or gender. However, a notable correlation was found with tumor grade ($p < 0.01$), T stage ($p < 0.05$), and pathological stage ($p < 0.05$) (Fig. 8). This analysis highlights the relevance of our SMRGs-based risk model, particularly in relation to tumor severity and progression in HNSCC, offering valuable insights for patient management and treatment planning.

3.8 TME and Immune Cell Infiltration are Predicted by the SMRGs Risk Score

We conducted an in-depth investigation into the relationship between the SMRGs risk score and the tumor microenvironment (TME) in HNSCC, focusing particularly on immune cell infiltration. Utilizing a comprehensive set of algorithms, including XCELL, QUANTISEQ, TIMER,

MCPCOUNTER, CIBERSORT-ABS, CIBERSORT, and EPIC (Fig. 9A), we sought to understand the complex dynamics within the TME. Our findings indicated a significant inverse relationship between the SMRGs risk score and the presence of various immune cells, including myeloid dendritic cells, T cells, CD8 T cells, B lineage cells, and NK cells (Fig. 9B). Moreover, single-sample Gene Set Enrichment Analysis (ssGSEA) revealed pronounced differences in immune function between high-risk (HR) and low-risk (LR) groups (Fig. 9C). A particularly striking discovery was the differential expression of immune checkpoints between the HR and LR groups. This aspect is of critical importance in the context of checkpoint-based immunotherapy. The LR group showed heightened expression of twelve immune checkpoint genes, notably including *LAIR1*, *IDO1*, *CTLA-4*, *PD-1*, *TIGIT*, *CD200R1*, *CEACAM1*, *CD200*, *KIR3DL*, *BTLA*, and *ADORA2A*, with a pronounced expression of *PD-1*. This pattern suggests a dependency on the PD-1/PD-L1 pathway for immune evasion in LR tumor cells (Fig. 9D), implying that treatments targeting PD-1 might be particularly effective in this subgroup. The activation of these immune checkpoints, such as PD-1, is typically associated with an inflamed TME [55], suggesting an in-

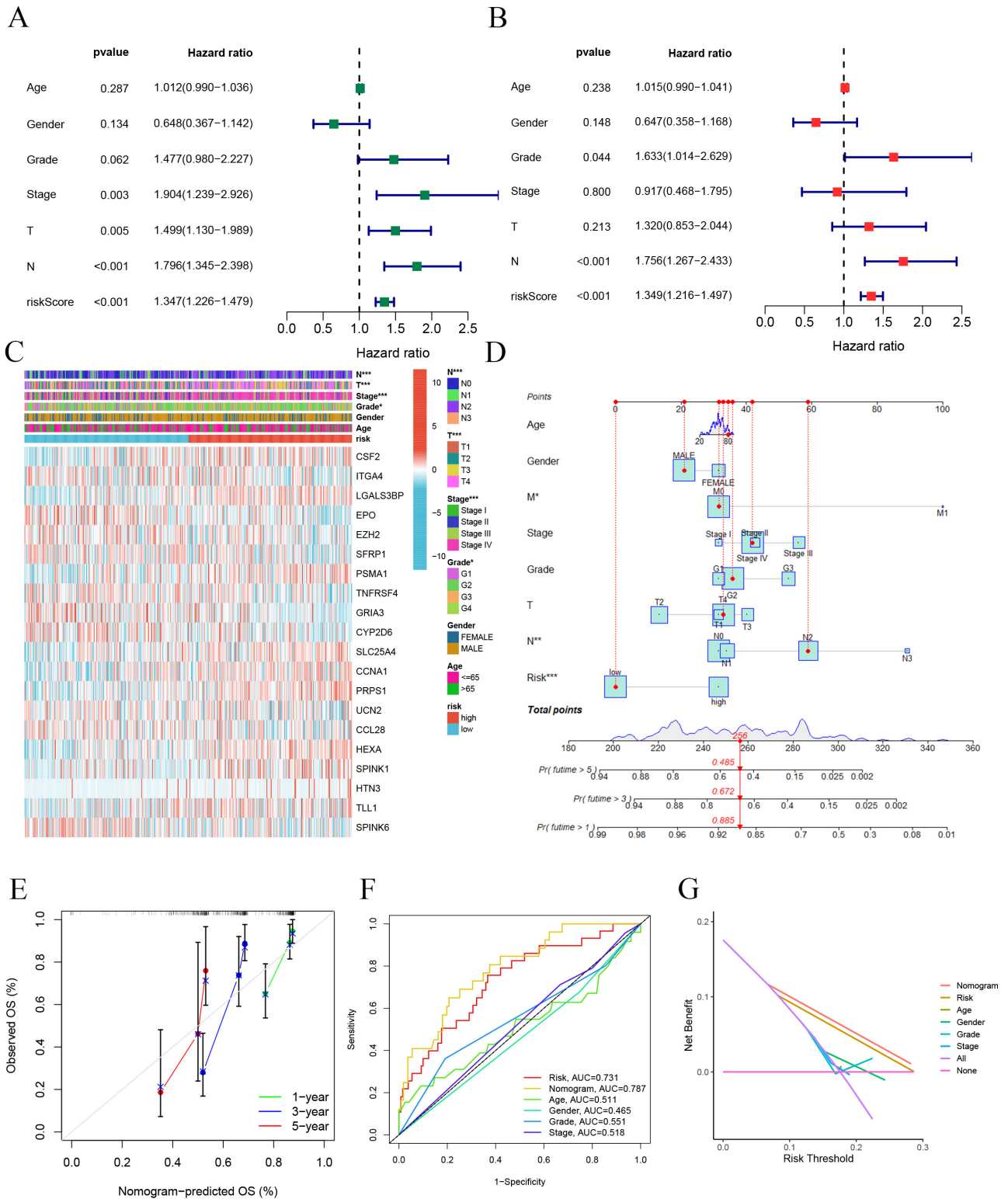


Fig. 6. Independent prognostic analysis of risk scores and clinical parameters. Univariate (A) and multivariate (B) COX regression analysis of the signature and different clinical features. (C) Heatmap for the 20 SMRGs-based signatures with clinicopathological manifestations. (D) Nomogram for predicting 1-year, 3-year, and 5-year OS of patients with HNSC. (E) The calibration curve of the constructed nomogram of 1-year, 3-year, and 5-year survival. (F) Multi-index ROC analysis in the test cohort. (G) Decision curve analysis. OS, overall survival; AUC, area under the curve.

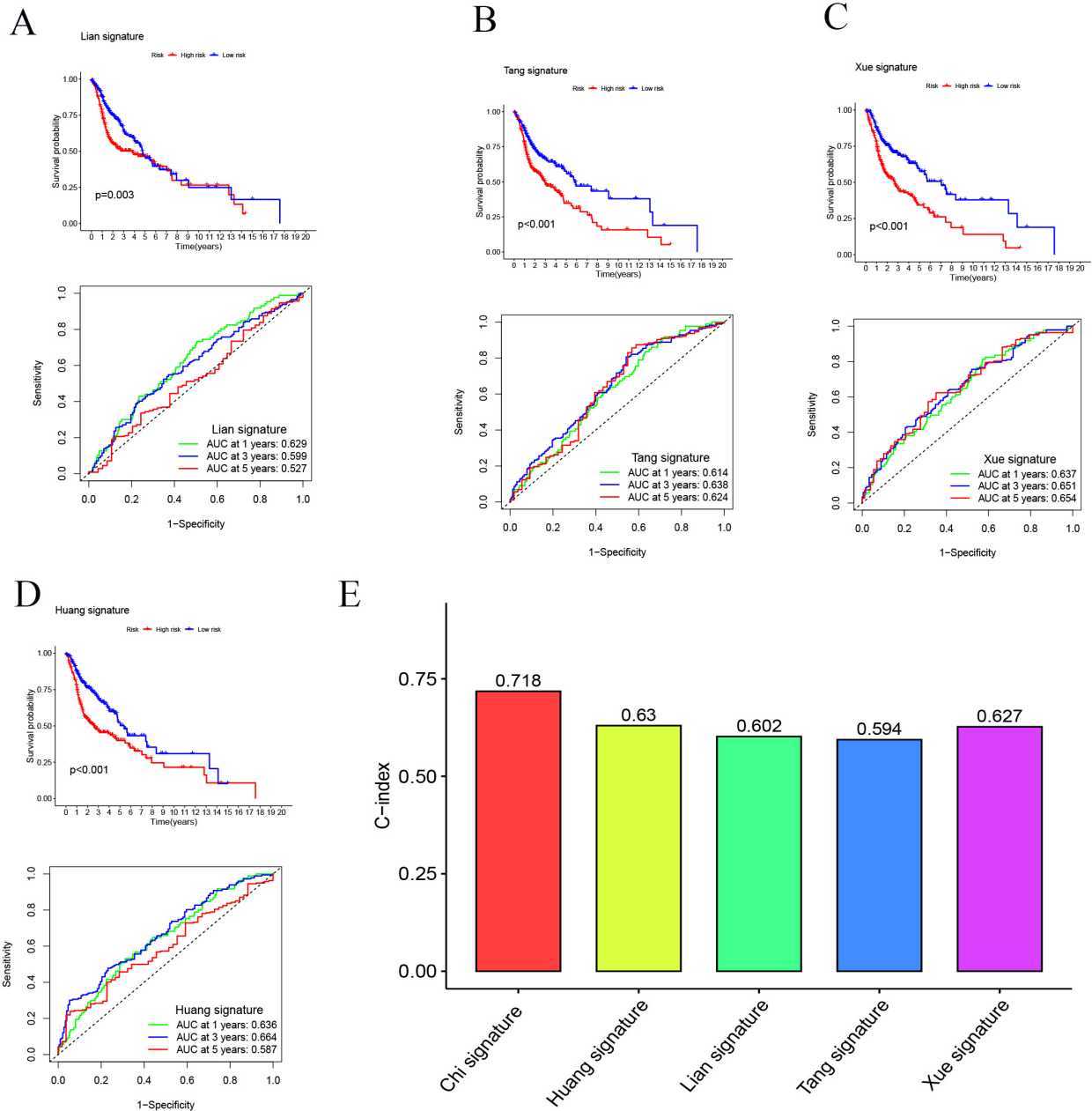


Fig. 7. Comparison of the SMRGs signature with other models. (A–D) Kaplan-Meier (K-M) curves and ROCs for risk models constructed by others. (E) C-indexes for five risk models.

inflammatory milieu in LR patients. Complementing this, our comparison of ssGSEA scores for various immune cells and functions revealed that all immune cell types, except for macrophages, were significantly more abundant in the LR group. Additionally, nine immune functions, including HLA and CCR, scored higher in the LR group (Fig. 9E,F). This comprehensive analysis underscores not only the robustness of our SMRGs risk score in prognostic prediction for HNSCC but also its significant implications in shaping personalized immunotherapeutic strategies. The insights garnered from this study could potentially guide more effective and tailored treatments for patients with HNSCC.

3.9 The Risk Score of the SMRG Predicts Immunotherapy Response

We initiated our analysis by exploring the Immunotherapy Prediction Pathway, focusing on the comparison between high-risk (HR) and low-risk (LR) groups. We discovered significant differences in several pathways (Fig. 10A). Notably, the LR group exhibited elevated Systemic lupus erythematosus risk scores, while other pathways such as Homologous recombination, Spliceosome, Progesterone-mediated oocyte maturation, and RNA degradation presented lower risk scores compared to the HR group (Fig. 10B). This suggests a better prognosis in the LR

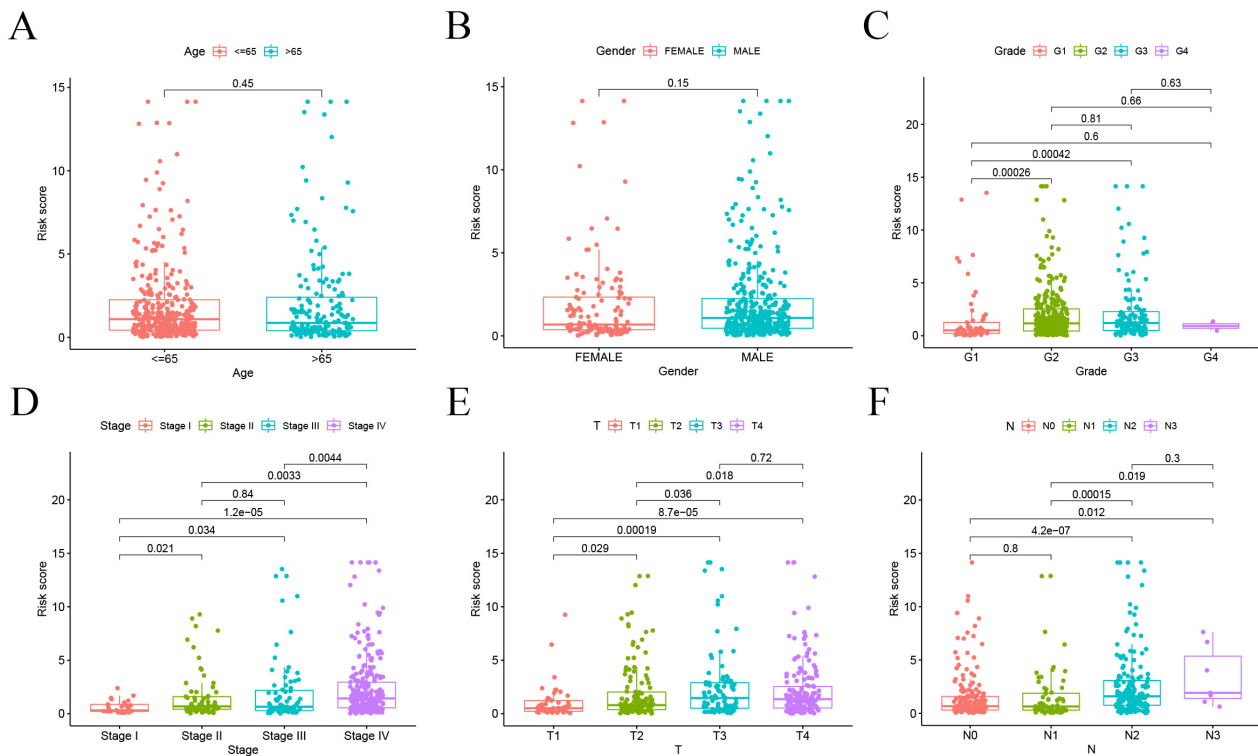


Fig. 8. Correlation analysis of risk scores and clinicopathological characteristics. (A) Age. (B) Gender. (C) Tumor grade. (D) Stage. (E) T stage. (F) N stage.

group, potentially influenced by aberrant RNA degradation processes impacting gene expression and cancer progression [56]. Further, we utilized the tumor immune cycle as a framework to evaluate the impact of immunomodulators and chemokine systems [44,57]. Our comparison of the HR and LR groups showed marked differences in the activities of various steps of the tumor immune cycle. Activities related to the expression of cancer cell antigen (step 2), initiation and activation (step 3), transport of immune cells to the tumor (step 4), infiltration into tumors (Step 5), recognition of cancer cells by T cells (Step 6), and the killing of cancer cells (step 7) were predominantly upregulated in the LR group. In contrast, the release of cancer cell antigens (step 1) demonstrated decreased activity (Fig. 10C). Analysis of risk scores related to these differences indicated higher scores in steps 3, 4, 5, 6, and 7 in the LR group, while other steps showed no significant variation (Fig. 10D).

Additionally, we explored the correlation between immune checkpoint blockade (ICB)-related signals and SMRG risk scores. This analysis revealed a negative correlation of the risk scores with pathways including DNA replication, Cell cycle, Fanconi anemia pathway, Homologous recombination, Nucleotide excision repair, Mismatch repair, Oocyte meiosis, Progesterone-mediated oocyte maturation, Spliceosome, Pyrimidine metabolism, and Systemic lupus erythematosus, while a positive correlation was observed with RNA degradation. Other pathways did not show significant correlations (Fig. 10E). Moreover, we

found that SMRG risk scores were inversely related to most tumor immune processes, except for cancer cell antigen release, Th22, eosinophil, neutrophil, basophil, or MDSC cell recruitment (Fig. 10E). Finally, our analysis using the BEST database demonstrated that the SMRGs Score has high sensitivity in predicting responses to immunotherapy in cancer patients (Fig. 10F–J). This finding provides valuable insights into the potential of SMRGs as a tool for guiding immunotherapeutic strategies, underscoring the significance of our comprehensive approach in understanding and predicting HNSCC treatment outcomes.

3.10 Differences in IC50 of Immunotherapy Drugs by Risk Score

A.770041 ($p = 3.4 \times 10^{-13}$), AS601245 ($p = 6.9 \times 10^{-10}$), AZ628 ($p = 4.8 \times 10^{-11}$), and AZD.0530 ($p = 1.9 \times 10^{-5}$) had greater IC50s in the LR group compared to the HR group when used to treat HNSC, out of a total of nine immunotherapeutic agents (Fig. 11A,F,H,I). The IC50 for the other 5 chemical or targeted medicines was lower in the LR group: ABT.263 ($p = 0.024$), ABT.888 ($p = 2.1 \times 10^{-7}$), AICAR ($p = 5.4 \times 10^{-6}$), AKT inhibitor VIII ($p = 1.9 \times 10^{-7}$), and ATRA ($p = 9.1 \times 10^{-11}$) (Fig. 11B,C,D,E,G). The risk score allows for more in-depth research into the immunotherapy response in HNSC patients and more targeted medication therapy.

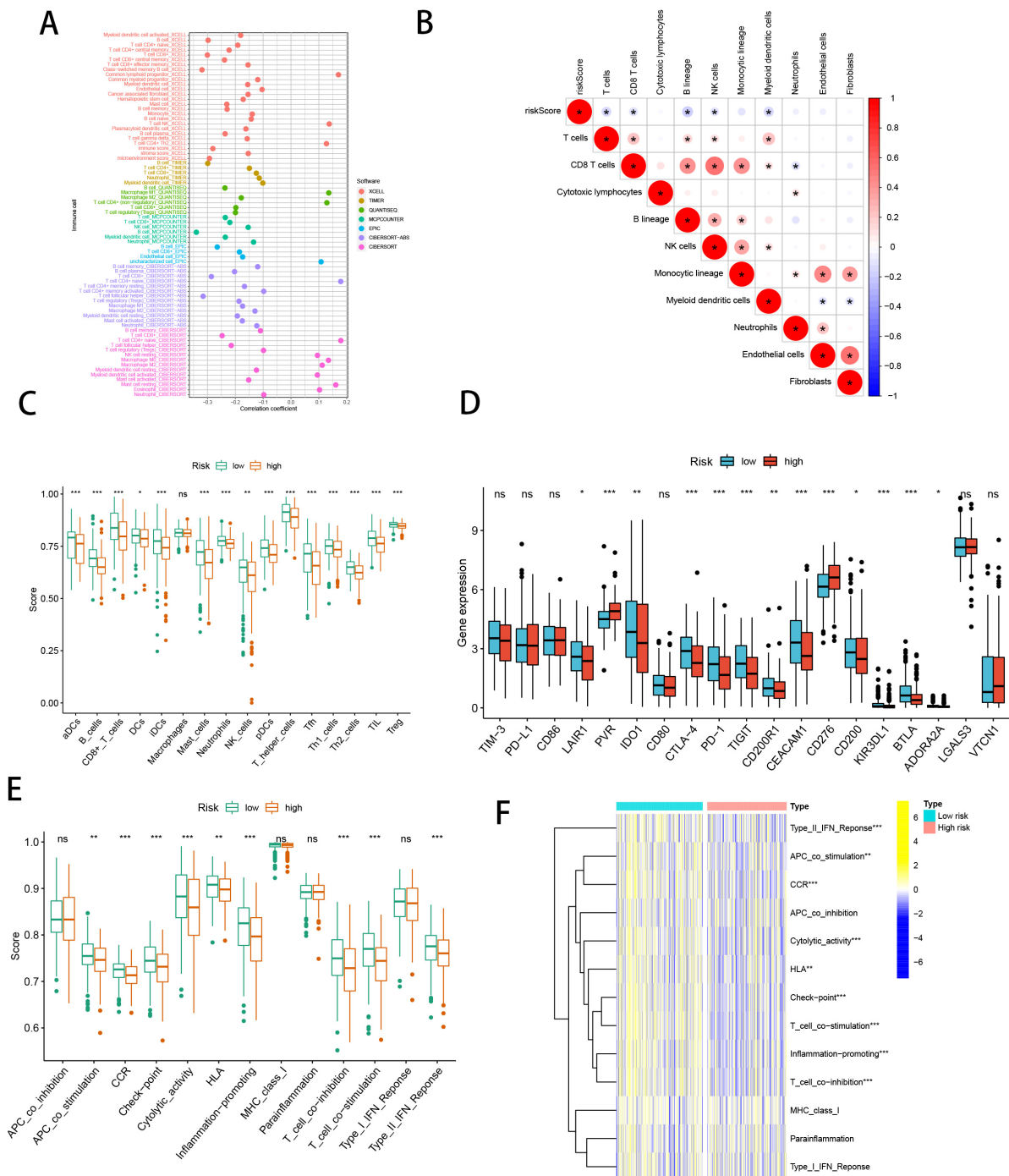


Fig. 9. SMRGs risk score predicts tumor microenvironment and immune cell infiltration. (A) Immune cell bubble plots. (B) The risk score and immune cell correlation. (C) Immune cell ssGSEA scores between high and low-risk groups. (D) Immune checkpoint differences between high and low-risk groups. (E) Immune function ssGSEA scores between high and low-risk groups. (F) Heat map of immune function differences between high- and low-risk groups. * $p < 0.05$; ** $p < 0.01$; *** $p < 0.001$. ssGSEA, single-sample Gene Set Enrichment Analysis; ns, not significant.

3.11 Correlation Analysis of SMRGs and TME

We leveraged the single-cell dataset HNSC GSE103322 from the TISCH database to explore the expression profiles of 20 selected SMRGs in tumor microenvironment (TME)-related cells. The dataset en-

compasses 20 distinct cell clusters, representing 11 unique cell types, as detailed in Fig. 12A. Our analysis revealed a varied expression pattern of SMRGs among different cell types. Notably, a spectrum of immune cells, including proliferating T, myofibroblasts, CD8⁺ T, CD4⁺ T, and

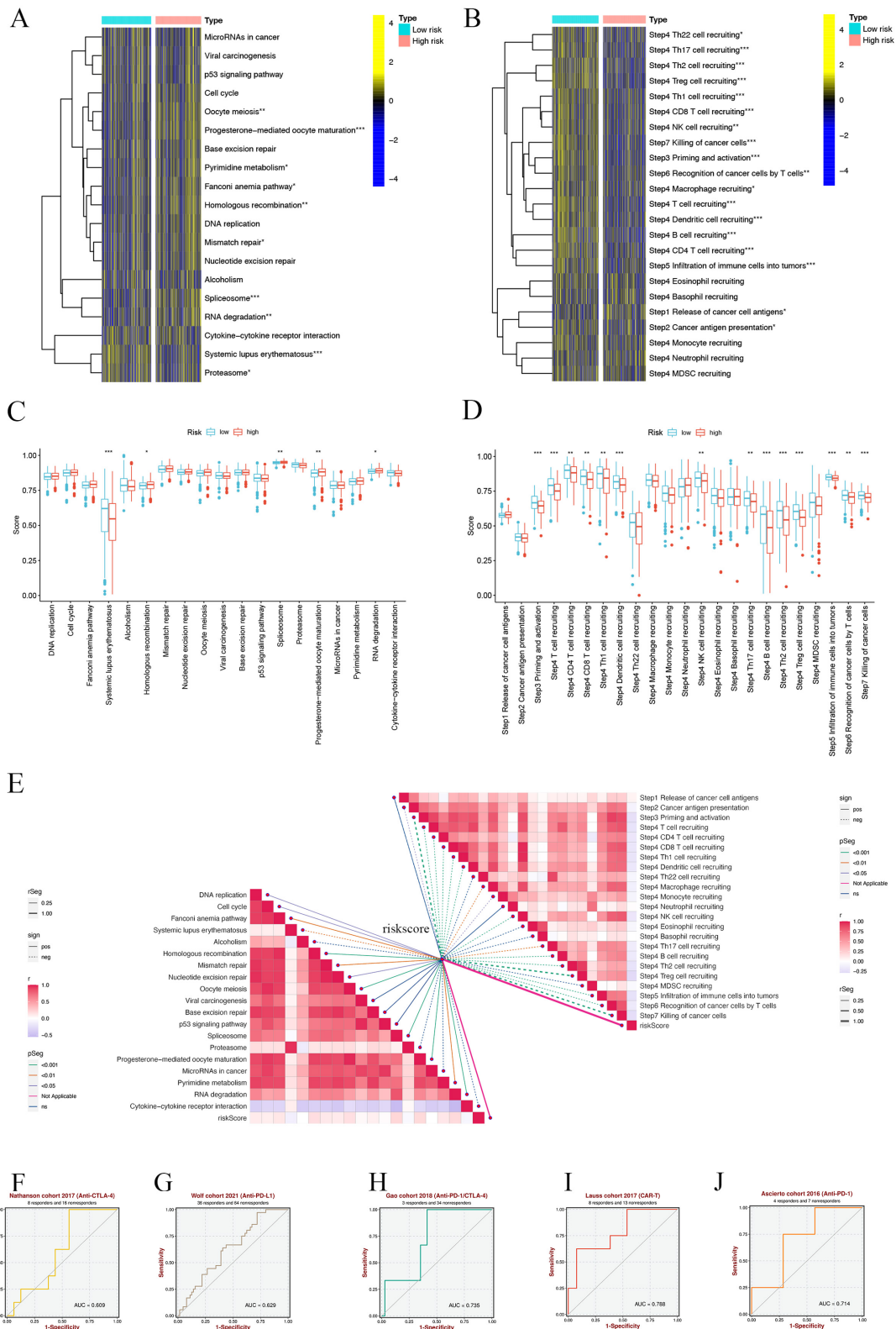


Fig. 10. SMRGs risk scores predicting treatment response assessment. (A) Heat map of the difference in enrichment scores between high and low-risk groups on the immunotherapy prediction pathway. (B) Heat map of differences between high and low-risk groups on each step of the cancer-immune cycle. (C) Differences in risk scores of immunotherapy prediction pathway between high and low-risk groups. (D) Differences in risk scores between high- and low-risk groups at steps of the cancer-immune cycle. (E) Correlation of different risk scores with the corresponding signals at the cancer-immune cycle step and ICB. (F–J) Sensitivity analysis of SMRGs score in predicting immunotherapy response to cancer. * $p < 0.05$; ** $p < 0.01$; *** $p < 0.001$. ICB, immune checkpoint blockade.

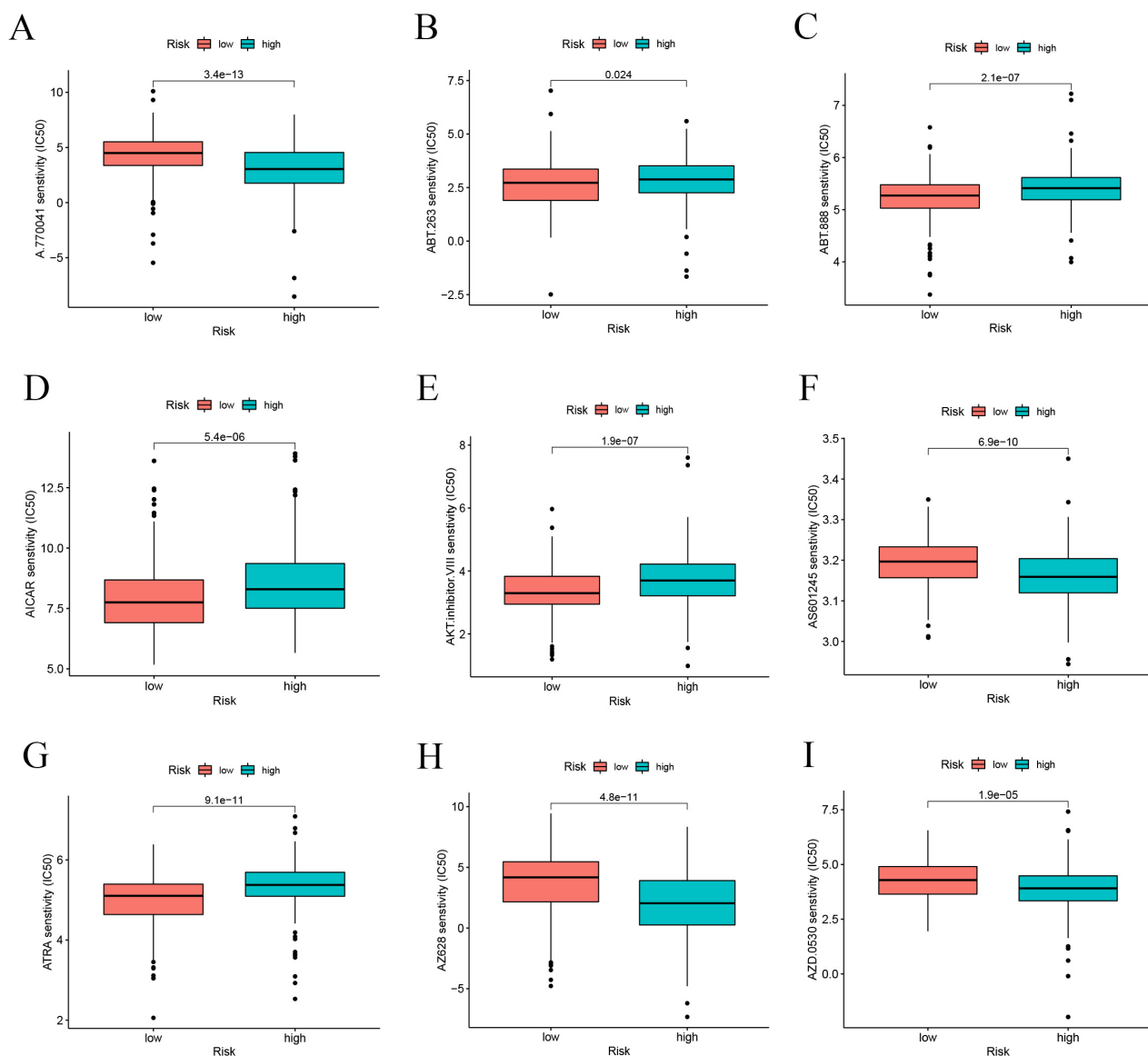


Fig. 11. Differences in IC50 of immunotherapy drugs by risk score. (A) A.770041. (B) ABT.263. (C) ABT.888. (D) AICAR. (E) AKT.inhibitor.VIII. (F) AS601245. (G) ATRA. (H) AZ628. (I) AZD.0530. IC50, half-maximal inhibitory concentration.

B cells, exhibited pronounced expression of LGALS3BP, PSMA1, HEXA, and PRPS1. Conversely, malignant cells predominantly expressed SPINK6, TLL1, UCN2, CCNA1, EPO, and CCL28. Proliferating T cells were characterized by elevated levels of ITGA4, TNFRSF4, PRPS1, and CYP2D6. Additionally, we observed a heterogeneous expression of PSMA1 and EZH2 across various immune cell types. LGALS3BP and HEXA, while displaying low to moderate expression in several immune cell populations, were markedly expressed in fibroblasts, myofibroblasts, and malignant cells. Furthermore, SFRP1 was notably present in fibroblast cells, whereas SLC25A4 was primarily found in myofibroblasts. Lastly, fibroblasts and cancer cells exhibited substantial expression of CSF2, GRIA3, HTN3, and SPINK1 (Fig. 12B, Supplementary Fig. 3).

3.12 Immunohistochemical Analysis was Used to Verify Gene Expression.

To further validate gene expression, we used immunohistochemical analysis. The results showed that LGALS3BP, EZH2, SFRP1, CCNA1 and SPRINK1 were highly expressed in HNSCC, while SLC25A4 was highly expressed in normal samples (Fig. 13).

4. Discussion

In this comprehensive study, we delve into the aggressive nature of HNSCC, a malignancy with a grim prognosis in advanced stages. Recent advancements, particularly in single-cell analyses targeting HNSC, have underscored the pivotal role of the tumor microenvironment (TME) in tumorigenesis [58,59]. Various cell populations

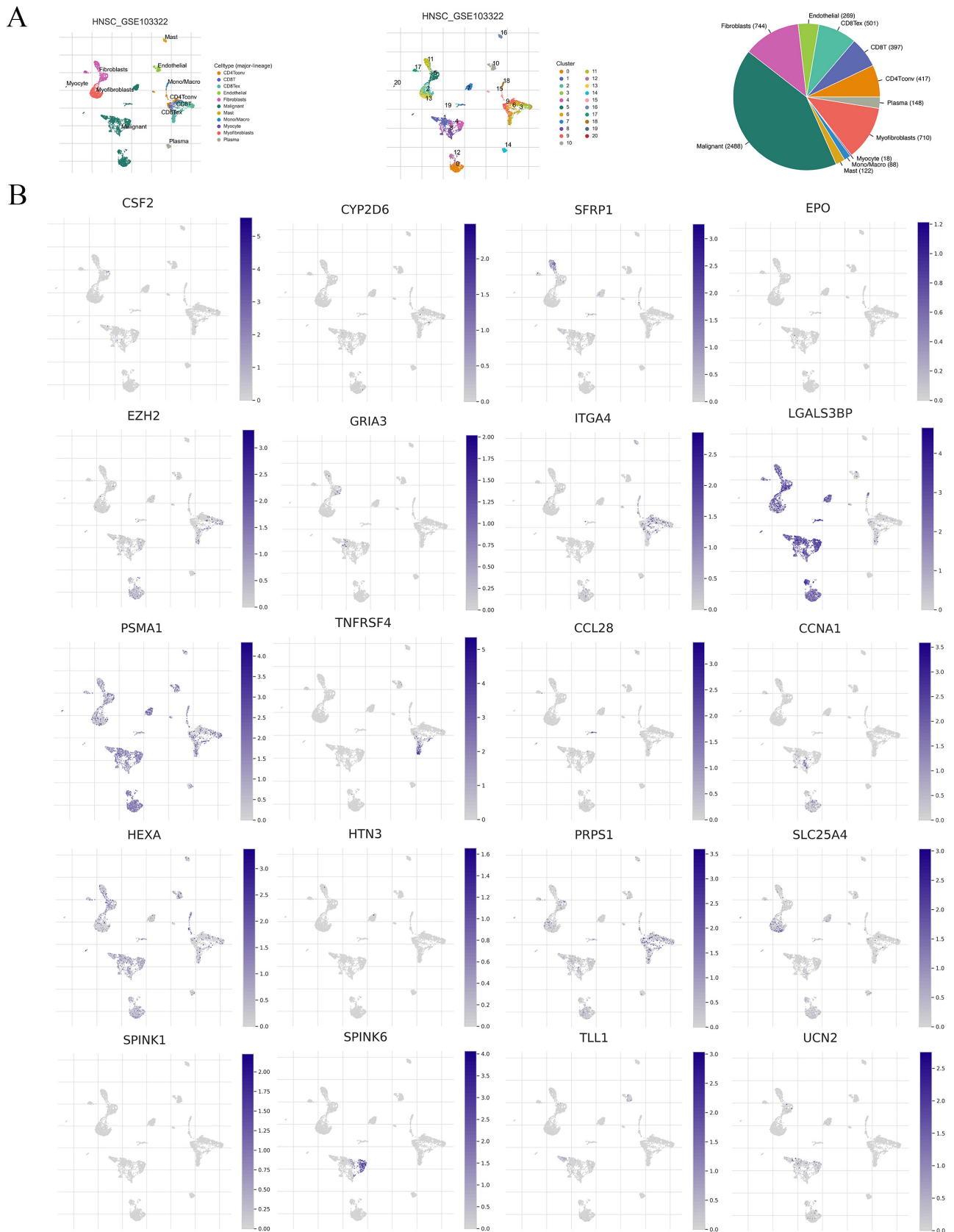


Fig. 12. SMRGs Expression in HNSCC TME-associated cells. (A) Annotation of all cell types in GSE103322 and the percentage of each cell type. (B) Percentages and expression of 20 SMRGs in different cell types in GSE103322. TME, tumor microenvironment.

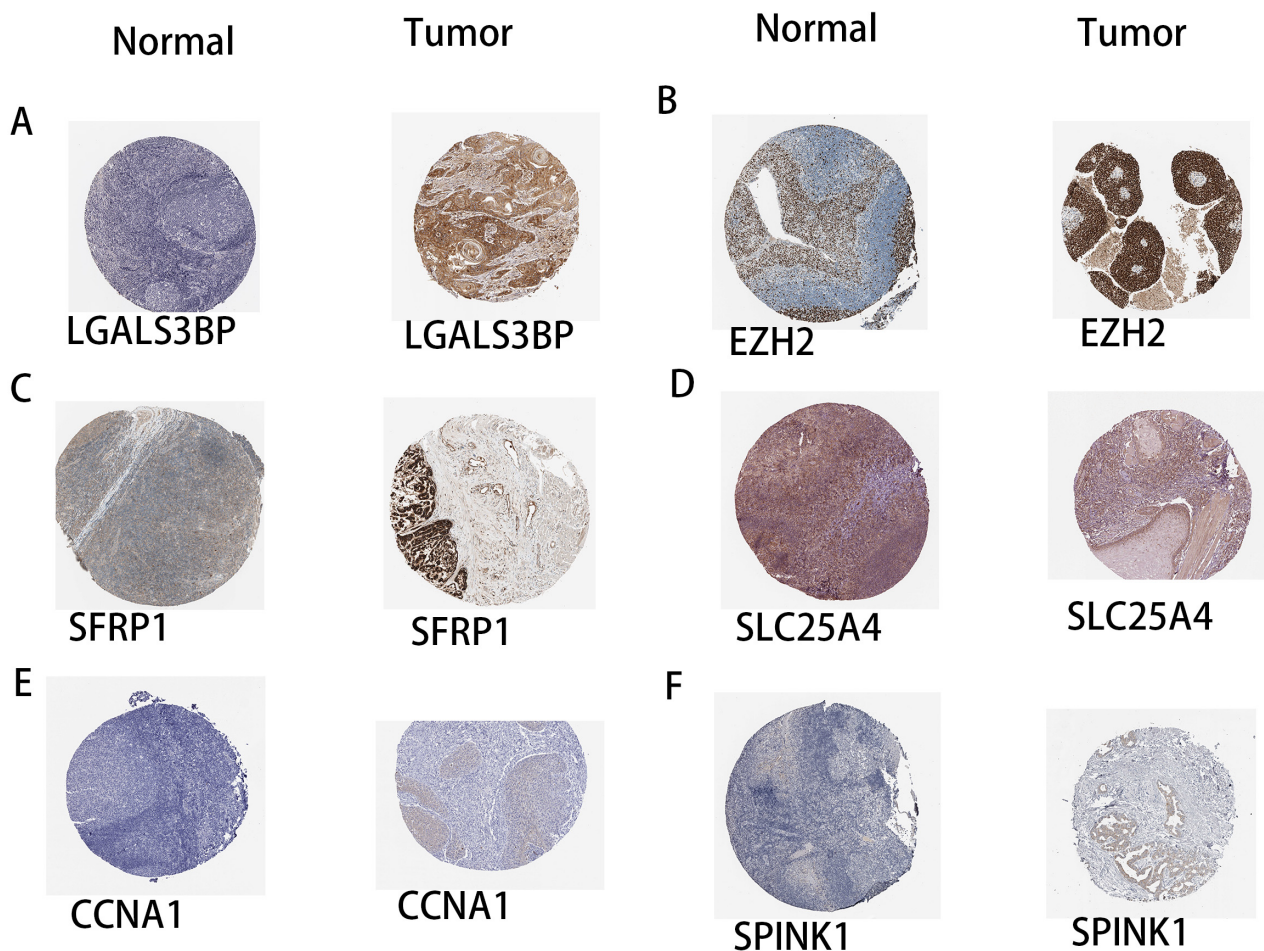


Fig. 13. Immunohistochemical analysis was used to verify gene expression. (A) LGALS3BP. (B) EZH2. (C) SFRP1. (D) SLC25A4. (E) CCNA1. (F) SPRINK1. Images available from <https://www.proteinatlas.org/ENSG00000108679-LGALS3BP/pathology/head+and+neck+cancer#img>. Light yellow, weak positivity; brownish yellow, moderate positivity; brownish black, strong positivity

within the TME secrete a plethora of soluble mediators, including chemokines, that sculpt the TME dynamics [60–63]. Furthermore, the burgeoning field of immunotherapy has shifted focus towards immune checkpoints, encompassing early diagnosis, combination therapies, and prediction of patient responses to treatment [64–66], with soluble immune checkpoint markers emerging as predictive indicators for response to immune checkpoint blockade (ICB) therapy [67].

Soluble mediators, including chemokines, Hsp70 family proteins, soluble sugars, lymphokines, and others, predominantly enter the extracellular compartment via exosomal vesicles [68–74]. Their extensive involvement in tumor progression and impact on patient prognosis is evident yet underexplored [75–78]. Our investigation focused on differentially expressed genes (DEGs) of soluble mediators in HNSCC, revealing their concentration in areas related to stromal tissue, humoral immune response, T cell activation, and regulation of lymphocyte activity. This indicates a strong immunological function association of these genes. Cluster analysis based on DE-SMRG highlighted signifi-

cant immune infiltration and survival differences among groups. Notably, prognostic clusters exhibited substantial infiltration of NK and CD8 T cells, key players in combating HNSC [79–82]. Previous studies have shown that CD8 T cell activation enhances radiotherapy efficacy in HNSC [83] and boosts NK and T cell effector functions [79,84,85]. Meta-analysis further supports the association of the NK cell ligand Fas with improved HNSC patient survival [86].

Our study constructs a multi-gene signature based on soluble mediator-related genes, proving effective in prognostic assessment for HNSC patients. Risk scores were calculated for each patient, categorizing them into high-risk (HR) and low-risk (LR) groups based on the expression levels of this signature. A nomogram incorporating clinicopathological criteria was developed, with decision curve analysis (DCA) demonstrating its clinical utility over single-factor models. This tool enables clinicians to tailor HNSC treatment strategies based on individual patient profiles.

Investigating immune infiltration levels across different risk groups, we found that the LR group showed higher

levels of immune cell infiltration, suggesting our model's efficacy in distinguishing 'cold' and 'hot' tumor subtypes in HNSC, with 'hot' subtypes indicating a more favorable prognosis. Given the potential of immune checkpoint inhibitors (ICIs) in HNSC treatment, particularly as primary treatments in advanced stages [87], the findings are significant. For instance, CD276 is highly expressed in CSCs in human HNSC, with elevated levels in the HR group correlating with reduced immune infiltration and immune evasion [88]. This underscores the need for combination immunotherapies in the HR group [89]. Targeting immune checkpoints like IDO1, PD-1, CEACAM1, and TIGIT, which show raised expression in the LR group, could benefit patients in this subset [90–92]. This hypothesis gains further credibility from immunotherapy response assessments across two risk subtypes using data from the BEST database.

The TME's complexity is evident from its diverse cell populations, including platelets, immune cells, and cancer-associated fibroblasts, all interconnected through soluble mediators [58,93–96]. Single-cell data analysis has enhanced our understanding of the distribution of soluble mediators across these cells. We observed significant enrichment of LGALS3BP, PSMA1, HEXA, and PRPS1 in various immune cells, including proliferating T, CD4⁺ T, and B cells. In contrast, CSF2, GRIA3, HTN3, and SPINK1 were mainly found in fibroblasts and malignant cells. The crucial role of cancer-associated fibroblasts in tumor progression has been established [97–99], suggesting these mediators as potential targets for HNSC treatment.

The granularity and spatial heterogeneity inherent in single-cell analyses have significantly enhanced our understanding of soluble mediators' roles in HNSCC. By focusing on these finer details, our study elucidates how soluble mediator-related gene (SMRG) expression impacts HNSCC prognosis and progression. The strength of our findings primarily lies in the predictive accuracy of the SMRG risk score and the derived nomogram. However, it's important to note that the current study's dataset is limited in size, necessitating future calibration of the prediction model with larger datasets for robustness. Moreover, the assessment of the signature's efficacy in predicting immunotherapy responses was conducted indirectly, due to the absence of mRNA expression profile data from HNSCC patients undergoing such treatments. This approach, while necessary, may not fully represent real-world scenarios. Consequently, future research should integrate data from HNSCC patients who have received immunotherapy to validate and refine our findings.

In clinical practice, the developed nomogram offers a valuable tool for physicians, enabling the creation of personalized treatment plans for HNSCC patients. The predictive accuracy of our multi-gene model in determining patient survival underscores its potential in guiding precision medicine. Going forward, in-depth research into the molec-

ular mechanisms underlying the actions of these therapeutically relevant soluble mediators, coupled with prospective randomized clinical trials, will be pivotal in advancing patient-specific therapeutic strategies and improving outcomes in HNSCC.

Acknowledging the limitations of our research is crucial for advancing our understanding and application of the findings in clinical settings. Primarily, our study's reliance on the TCGA dataset, while extensive, encounters constraints due to the inherent biases and data limitations of available mRNA information. Our efforts to validate the findings with external datasets are commendable, yet they fall short of capturing a comprehensive real-world scenario. To bolster the credibility and applicability of our prognostic model, future validations must integrate a broader spectrum of real-world data. Secondly, the inclusion of 20 SMRGs as independent prognostic variables for HNSCC was intended to enhance the model's specificity and accuracy. Nevertheless, this approach might impose a financial burden on patients due to the costs associated with comprehensive gene profiling. Addressing this concern is imperative to not only enhance the model's practicality but also to ensure its equitable application across diverse patient populations. As we progress in our research, refining our methodologies to overcome these challenges will be vital for improving the clinical utility and relevance of our findings in the treatment of HNSCC.

5. Conclusions

In conclusion, our study represents a systematic exploration of SMRGs in the context of HNSCC. We have successfully developed a prognostic signature comprising 20 SMRGs. This signature stands out for its ability to accurately evaluate the prognosis and immune status of HNSCC patients. Crucially, it equips clinicians with a powerful tool to identify specific patient subgroups who are likely to respond favorably to immunotherapy and chemotherapy. The application of this signature in clinical settings promises to enhance the personalization of treatment strategies, tailoring them to the unique molecular and immunological landscapes of individual HNSCC cases.

Availability of Data and Materials

The datasets in this study were obtained from the TCGA database (<http://cancergenome.nih.gov/>), and ICGC database (<https://dcc.icgc.org>).

Author Contributions

HC, QW, KX, and GY conceived the study. HC, GP, GS, JinZ, XX, JY, JX and JieZ drafted the manuscript. HC, XX, JY, JieZ and JX performed the literature search and collected the data. HC, GP, GS and JinZ analyzed and visualized the data. QW and GY revised the manuscript and was a supporter of the study. All authors contributed to ed-

itorial changes in the manuscript. All authors read and approved the final manuscript. All authors have participated sufficiently in the work and agreed to be accountable for all aspects of the work.

Ethics Approval and Consent to Participate

This study adhered to public database guidelines and data access policies, and approval by the local ethics committees was not required.

Acknowledgment

Not applicable.

Funding

This study was supported by grants from the Science and Technology Development Fund, Macau SAR (No.: 0098/2021/A2 and 0048/2023/AFJ), Macau University of Science and Technology's Faculty Research Grant (No: FRG-23-003-FC).

Conflict of Interest

The authors declare no conflict of interest.

Supplementary Material

Supplementary material associated with this article can be found, in the online version, at <https://doi.org/10.31083/j.fbl2903130>.

References

- [1] Leemans CR, Braakhuis BJM, Brakenhoff RH. The molecular biology of head and neck cancer. *Nature Reviews. Cancer*. 2011; 11: 9–22.
- [2] Chi H, Jiang P, Xu K, Zhao Y, Song B, Peng G, *et al.* A novel anoikis-related gene signature predicts prognosis in patients with head and neck squamous cell carcinoma and reveals immune infiltration. *Frontiers in Genetics*. 2022; 13: 984273.
- [3] Fitzmaurice C, Allen C, Barber RM, Barregard L, Bhutta ZA, Brenner H, *et al.* Global, regional, and national cancer incidence, mortality, years of life lost, years lived with disability, and disability-adjusted life-years for 32 cancer groups, 1990 to 2015: a systematic analysis for the global burden of disease study. *JAMA Oncology*. 2017; 3: 524–548.
- [4] Liang F, Wang R, Du Q, Zhu S. An Epithelial-Mesenchymal Transition Hallmark Gene-Based Risk Score System in Head and Neck Squamous-Cell Carcinoma. *International Journal of General Medicine*. 2021; 14: 4219–4227.
- [5] Valjevac A, Dzubur A, Nakas-Icindic E, Hadzovic-Dzuvu A, Lepara O, Kiseljakovic E, *et al.* Is γ -glutamyl transferase activity a potential marker of left ventricular function during early postmyocardial infarction period? *Future Cardiology*. 2011; 7: 705–713.
- [6] Ribeiro IP, Caramelo F, Esteves L, Menoita J, Marques F, Barroso L, *et al.* Genomic predictive model for recurrence and metastasis development in head and neck squamous cell carcinoma patients. *Scientific Reports*. 2017; 7: 13897.
- [7] Chi H, Yang J, Peng G, Zhang J, Song G, Xie X, *et al.* Circadian rhythm-related genes index: A predictor for HNSCC prognosis, immunotherapy efficacy, and chemosensitivity. *Frontiers in Immunology*. 2023; 14: 1091218.
- [8] Lee CC, Ho HC, Su YC, Yu CH, Yang CC. Modified Tumor Classification With Inclusion of Tumor Characteristics Improves Discrimination and Prediction Accuracy in Oral and Hypopharyngeal Cancer Patients Who Underwent Surgery. *Medicine*. 2015; 94: e1114.
- [9] Takes RP, Rinaldo A, Silver CE, Piccirillo JF, Haigentz M, Jr, Suárez C, *et al.* Future of the TNM classification and staging system in head and neck cancer. *Head & Neck*. 2010; 32: 1693–1711.
- [10] Raz Y, Erez N. An inflammatory vicious cycle: Fibroblasts and immune cell recruitment in cancer. *Experimental Cell Research*. 2013; 319: 1596–1603.
- [11] Tabolacci C, Cordella M, Mariotti S, Rossi S, Senatore C, Lintas C, *et al.* Melanoma Cell Resistance to Vemurafenib Modifies Inter-Cellular Communication Signals. *Biomedicines*. 2021; 9: 79.
- [12] Schaaf MB, Garg AD, Agostinis P. Defining the role of the tumor vasculature in antitumor immunity and immunotherapy. *Cell Death & Disease*. 2018; 9: 115.
- [13] Lehnert BE, Goodwin EH, Deshpande A. Extracellular factor(s) following exposure to alpha particles can cause sister chromatid exchanges in normal human cells. *Cancer Research*. 1997; 57: 2164–2171.
- [14] Shao C, Furusawa Y, Aoki M, Matsumoto H, Ando K. Nitric oxide-mediated bystander effect induced by heavy-ions in human salivary gland tumour cells. *International Journal of Radiation Biology*. 2002; 78: 837–844.
- [15] Shao C, Stewart V, Folkard M, Michael BD, Prise KM. Nitric oxide-mediated signaling in the bystander response of individually targeted glioma cells. *Cancer Research*. 2003; 63: 8437–8442.
- [16] Chou CH, Chen PJ, Lee PH, Cheng AL, Hsu HC, Cheng JCH. Radiation-induced hepatitis B virus reactivation in liver mediated by the bystander effect from irradiated endothelial cells. *Clinical Cancer Research: an Official Journal of the American Association for Cancer Research*. 2007; 13: 851–857.
- [17] Narayanan PK, LaRue KE, Goodwin EH, Lehnert BE. Alpha particles induce the production of interleukin-8 by human cells. *Radiation Research*. 1999; 152: 57–63.
- [18] Iyer R, Lehnert BE, Svensson R. Factors underlying the cell growth-related bystander responses to alpha particles. *Cancer Research*. 2000; 60: 1290–1298.
- [19] Zhou H, Ivanov VN, Gillespie J, Geard CR, Amundson SA, Brenner DJ, *et al.* Mechanism of radiation-induced bystander effect: role of the cyclooxygenase-2 signaling pathway. *Proceedings of the National Academy of Sciences of the United States of America*. 2005; 102: 14641–14646.
- [20] Tong CCL, Kao J, Sikora AG. Recognizing and reversing the immunosuppressive tumor microenvironment of head and neck cancer. *Immunologic Research*. 2012; 54: 266–274.
- [21] Eckert AW, Wickenhauser C, Salins PC, Kappler M, Bukur J, Seliger B. Clinical relevance of the tumor microenvironment and immune escape of oral squamous cell carcinoma. *Journal of Translational Medicine*. 2016; 14: 85.
- [22] Jin J, Si J, Liu Y, Wang H, Ni R, Wang J. Elevated serum soluble programmed cell death ligand 1 concentration as a potential marker for poor prognosis in small cell lung cancer patients with chemotherapy. *Respiratory Research*. 2018; 19: 197.
- [23] Wang H, Wang L, Liu WJ, Xia ZJ, Huang HQ, Jiang WQ, *et al.* High post-treatment serum levels of soluble programmed cell death ligand 1 predict early relapse and poor prognosis in extranodal NK/T cell lymphoma patients. *Oncotarget*. 2016; 7: 33035–33045.
- [24] Guo X, Wang J, Jin J, Chen H, Zhen Z, Jiang W, *et al.* High Serum Level of Soluble Programmed Death Ligand 1 is Asso-

- ciated With a Poor Prognosis in Hodgkin Lymphoma. *Translational Oncology*. 2018; 11: 779–785.
- [25] Ding D, Song Y, Yao Y, Zhang S. Preoperative serum macrophage activated biomarkers soluble mannose receptor (sMR) and soluble haemoglobin scavenger receptor (sCD163), as novel markers for the diagnosis and prognosis of gastric cancer. *Oncology Letters*. 2017; 14: 2982–2990.
- [26] Smyth GK. Linear models and empirical bayes methods for assessing differential expression in microarray experiments. *Statistical Applications in Genetics and Molecular Biology*. 2004; 3: Article3.
- [27] Shen Y, Chi H, Xu K, Li Y, Yin X, Chen S, *et al.* A Novel Classification Model for Lower-Grade Glioma Patients Based on Pyroptosis-Related Genes. *Brain Sciences*. 2022; 12: 700.
- [28] Zhao S, Zhang L, Ji W, Shi Y, Lai G, Chi H, *et al.* Machine learning-based characterization of cuproptosis-related biomarkers and immune infiltration in Parkinson's disease. *Frontiers in Genetics*. 2022; 13: 1010361.
- [29] Yu G, Wang LG, Han Y, He QY. clusterProfiler: an R package for comparing biological themes among gene clusters. *Omic: a Journal of Integrative Biology*. 2012; 16: 284–287.
- [30] Li XY, Zhao ZJ, Wang JB, Shao YH, Hui-Liu, You JX, *et al.* m7G Methylation-Related Genes as Biomarkers for Predicting Overall Survival Outcomes for Hepatocellular Carcinoma. *Frontiers in Bioengineering and Biotechnology*. 2022; 10: 849756.
- [31] Wilkerson MD, Hayes DN. ConsensusClusterPlus: a class discovery tool with confidence assessments and item tracking. *Bioinformatics (Oxford, England)*. 2010; 26: 1572–1573.
- [32] Dienstmann R, Villacampa G, Sveen A, Mason MJ, Niedzwiecki D, Nesbakken A, *et al.* Relative contribution of clinicopathological variables, genomic markers, transcriptomic subtyping and microenvironment features for outcome prediction in stage II/III colorectal cancer. *Annals of Oncology: Official Journal of the European Society for Medical Oncology*. 2019; 30: 1622–1629.
- [33] Friedman J, Hastie T, Tibshirani R. Regularization Paths for Generalized Linear Models via Coordinate Descent. *Journal of Statistical Software*. 2010; 33: 1–22.
- [34] Longato E, Vettoretti M, Di Camillo B. A practical perspective on the concordance index for the evaluation and selection of prognostic time-to-event models. *Journal of Biomedical Informatics*. 2020; 108: 103496.
- [35] Zhao Z, Ding Y, Tran LJ, Chai G, Lin L. Innovative breakthroughs facilitated by single-cell multi-omics: manipulating natural killer cell functionality correlates with a novel subcategory of melanoma cells. *Frontiers in Immunology*. 2023; 14: 1196892.
- [36] Aran D, Hu Z, Butte AJ. xCell: digitally portraying the tissue cellular heterogeneity landscape. *Genome Biology*. 2017; 18: 220.
- [37] Aran D. Cell-Type Enrichment Analysis of Bulk Transcriptomes Using xCell. *Methods in Molecular Biology (Clifton, N.J.)*. 2020; 2120: 263–276.
- [38] Chen B, Khodadoust MS, Liu CL, Newman AM, Alizadeh AA. Profiling Tumor Infiltrating Immune Cells with CIBERSORT. *Methods in Molecular Biology (Clifton, N.J.)*. 2018; 1711: 243–259.
- [39] Li T, Fu J, Zeng Z, Cohen D, Li J, Chen Q, *et al.* TIMER2.0 for analysis of tumor-infiltrating immune cells. *Nucleic Acids Research*. 2020; 48: W509–W514.
- [40] Plattner C, Finotello F, Rieder D. Deconvoluting tumor-infiltrating immune cells from RNA-seq data using quanTIseq. *Methods in Enzymology*. 2020; 636: 261–285.
- [41] Finotello F, Mayer C, Plattner C, Laschober G, Rieder D, Hackl H, *et al.* Molecular and pharmacological modulators of the tumor immune contexture revealed by deconvolution of RNA-seq data. *Genome Medicine*. 2019; 11: 34.
- [42] Racle J, de Jonge K, Baumgaertner P, Speiser DE, Gfeller D. Simultaneous enumeration of cancer and immune cell types from bulk tumor gene expression data. *eLife*. 2017; 6: e26476.
- [43] Zhang H, Li R, Cao Y, Gu Y, Lin C, Liu X, *et al.* Poor Clinical Outcomes and Immuno-evasive Contexture in Intratumoral IL-10-Producing Macrophages Enriched Gastric Cancer Patients. *Annals of Surgery*. 2022; 275: e626–e635.
- [44] Xu L, Deng C, Pang B, Zhang X, Liu W, Liao G, *et al.* TIP: A Web Server for Resolving Tumor Immunophenotype Profiling. *Cancer Research*. 2018; 78: 6575–6580.
- [45] Tamminga M, Hiltermann TJN, Schuurung E, Timens W, Fehrmann RS, Groen HJ. Immune microenvironment composition in non-small cell lung cancer and its association with survival. *Clinical & Translational Immunology*. 2020; 9: e1142.
- [46] Auslander N, Zhang G, Lee JS, Frederick DT, Miao B, Moll T, *et al.* Robust prediction of response to immune checkpoint blockade therapy in metastatic melanoma. *Nature Medicine*. 2018; 24: 1545–1549.
- [47] Mariathasan S, Turley SJ, Nickles D, Castiglioni A, Yuen K, Wang Y, *et al.* TGF β attenuates tumour response to PD-L1 blockade by contributing to exclusion of T cells. *Nature*. 2018; 554: 544–548.
- [48] Hänzelmann S, Castelo R, Guinney J. GSEA: gene set variation analysis for microarray and RNA-seq data. *BMC Bioinformatics*. 2013; 14: 7.
- [49] Geleher P, Cox NJ, Huang RS. Clinical drug response can be predicted using baseline gene expression levels and in vitro drug sensitivity in cell lines. *Genome Biology*. 2014; 15: R47.
- [50] Chi H, Gao X, Xia Z, Yu W, Yin X, Pan Y, *et al.* FAM family gene prediction model reveals heterogeneity, stemness and immune microenvironment of UCEC. *Frontiers in Molecular Biosciences*. 2023; 10: 1200335.
- [51] Zheng L, Guan Z, Xue M. TGF- β Signaling Pathway-Based Model to Predict the Subtype and Prognosis of Head and Neck Squamous Cell Carcinoma. *Frontiers in Genetics*. 2022; 13: 862860.
- [52] Tang X, Li R, Wu D, Wang Y, Zhao F, Lv R, *et al.* Development and Validation of an ADME-Related Gene Signature for Survival, Treatment Outcome and Immune Cell Infiltration in Head and Neck Squamous Cell Carcinoma. *Frontiers in Immunology*. 2022; 13: 905635.
- [53] Liu B, Su Q, Ma J, Chen C, Wang L, Che F, *et al.* Prognostic Value of Eight-Gene Signature in Head and Neck Squamous Carcinoma. *Frontiers in Oncology*. 2021; 11: 657002.
- [54] Huang J, Huo H, Lu R. A Novel Signature of Necroptosis-Associated Genes as a Potential Prognostic Tool for Head and Neck Squamous Cell Carcinoma. *Frontiers in Genetics*. 2022; 13: 907985.
- [55] Spranger S, Spaepen RM, Zha Y, Williams J, Meng Y, Ha TT, *et al.* Up-regulation of PD-L1, IDO, and T(regs) in the melanoma tumor microenvironment is driven by CD8(+) T cells. *Science Translational Medicine*. 2013; 5: 200ra116.
- [56] Liu J, Chen T, Yang M, Zhong Z, Ni S, Yang S, *et al.* Development of an Oxidative Phosphorylation-Related and Immune Microenvironment Prognostic Signature in Uterine Corpus Endometrial Carcinoma. *Frontiers in Cell and Developmental Biology*. 2021; 9: 753004.
- [57] Chen DS, Mellman I. Oncology meets immunology: the cancer-immunity cycle. *Immunity*. 2013; 39: 1–10.
- [58] Peltanova B, Raudenska M, Masarik M. Effect of tumor microenvironment on pathogenesis of the head and neck squamous cell carcinoma: a systematic review. *Molecular Cancer*. 2019; 18: 63.
- [59] Peng G, Chi H, Gao X, Zhang J, Song G, Xie X, *et al.* Identification and validation of neurotrophic factor-related genes signature in HNSCC to predict survival and immune landscapes.

Frontiers in Genetics. 2022; 13: 1010044.

- [60] Ozga AJ, Chow MT, Luster AD. Chemokines and the immune response to cancer. *Immunity*. 2021; 54: 859–874.
- [61] Nagarsheth N, Wicha MS, Zou W. Chemokines in the cancer microenvironment and their relevance in cancer immunotherapy. *Nature Reviews. Immunology*. 2017; 17: 559–572.
- [62] Li X, Liu Z, Zhou W, Liu X, Cao W. Downregulation of CCL22 and mutated NOTCH1 in tongue and mouth floor squamous cell carcinoma results in decreased Th2 cell recruitment and expression, predicting poor clinical outcome. *BMC Cancer*. 2021; 21: 922.
- [63] Zhang Y, Chen K, Li L, Mao W, Shen D, Yao N, *et al*. CCR4 is a prognostic biomarker and correlated with immune infiltrates in head and neck squamous cell carcinoma. *Annals of Translational Medicine*. 2021; 9: 1443.
- [64] Mazieres J, Drilon A, Lusque A, Mhanna L, Cortot AB, Mezquita L, *et al*. Immune checkpoint inhibitors for patients with advanced lung cancer and oncogenic driver alterations: results from the IMMUNOTARGET registry. *Annals of Oncology: Official Journal of the European Society for Medical Oncology*. 2019; 30: 1321–1328.
- [65] Bagchi S, Yuan R, Engleman EG. Immune Checkpoint Inhibitors for the Treatment of Cancer: Clinical Impact and Mechanisms of Response and Resistance. *Annual Review of Pathology*. 2021; 16: 223–249.
- [66] Lee CH, Shah AY, Rasco D, Rao A, Taylor MH, Di Simone C, *et al*. Lenvatinib plus pembrolizumab in patients with either treatment-naïve or previously treated metastatic renal cell carcinoma (Study 111/KEYNOTE-146): a phase 1b/2 study. *The Lancet. Oncology*. 2021; 22: 946–958.
- [67] Raza A, Mohsen R, Kanbour A, Zar Gul AR, Philip A, Vijayakumar S, *et al*. 17 Predictive soluble biomarkers of immune response to checkpoint blockade in non-small cell lung cancer (NSCLC) patients. *Journal for Immunotherapy of Cancer*. 2021; 9: A19.
- [68] De Wever O, Derycke L, Hendrix A, De Meerleer G, Godeau F, Depypere H, *et al*. Soluble cadherins as cancer biomarkers. *Clinical & Experimental Metastasis*. 2007; 24: 685–697.
- [69] Jirillo E, De Rinaldis P. Lymphokines: soluble mediators of the cellular immunity *in vitro* and *in vivo*. *Recenti Progressi in Medicina*. 1976; 61: 624–629.
- [70] Kent D, Vinoses SA, Campochiaro PA. Macular oedema: the role of soluble mediators. *The British Journal of Ophthalmology*. 2000; 84: 542–545.
- [71] Bertrand J, Bollmann M. Soluble syndecans: biomarkers for diseases and therapeutic options. *British Journal of Pharmacology*. 2019; 176: 67–81.
- [72] Levine SJ. Mechanisms of soluble cytokine receptor generation. *Journal of Immunology (Baltimore, Md.: 1950)*. 2004; 173: 5343–5348.
- [73] Grisaru-Tal S, Itan M, Klion AD, Munitz A. A new dawn for eosinophils in the tumour microenvironment. *Nature Reviews. Cancer*. 2020; 20: 594–607.
- [74] Kroemer G, Galluzzi L, Kepp O, Zitvogel L. Immunogenic cell death in cancer therapy. *Annual Review of Immunology*. 2013; 31: 51–72.
- [75] Shehzad A, Islam SU, Shahzad R, Khan S, Lee YS. Extracellular vesicles in cancer diagnostics and therapeutics. *Pharmacology & Therapeutics*. 2021; 223: 107806.
- [76] Fernandes JV, Cobucci RNO, Jatobá CAN, Fernandes TAADM, de Azevedo JWV, de Araújo JMG. The role of the mediators of inflammation in cancer development. *Pathology Oncology Research: POR*. 2015; 21: 527–534.
- [77] Kluckova K, Durmanova V, Bucova M. Soluble HLA-G, its diagnostic and prognostic value and potential target molecule for future therapy in cancer. *Bratislavské Lekárske Listy*. 2021; 122: 60–617.
- [78] Hu QP, Kuang JY, Yang QK, Bian XW, Yu SC. Beyond a tumor suppressor: Soluble E-cadherin promotes the progression of cancer. *International Journal of Cancer*. 2016; 138: 2804–2812.
- [79] André P, Denis C, Soulas C, Bourbon-Caillet C, Lopez J, Arnoux T, *et al*. Anti-NKG2A mAb Is a Checkpoint Inhibitor that Promotes Anti-tumor Immunity by Unleashing Both T and NK Cells. *Cell*. 2018; 175: 1731–1743.e13.
- [80] Hewavisenti R, Ferguson A, Wang K, Jones D, Gebhardt T, Edwards J, *et al*. CD103+ tumor-resident CD8+ T cell numbers underlie improved patient survival in oropharyngeal squamous cell carcinoma. *Journal for Immunotherapy of Cancer*. 2020; 8: e000452.
- [81] Budden T, Gaudy-Marqueste C, Craig S, Hu Y, Earnshaw CH, Gurung S, *et al*. Female Immunity Protects from Cutaneous Squamous Cell Carcinoma. *Clinical Cancer Research: an Official Journal of the American Association for Cancer Research*. 2021; 27: 3215–3223.
- [82] Hecht M, Eckstein M, Rutzner S, von der Grün J, Illmer T, Klautke G, *et al*. Induction chemoimmunotherapy followed by CD8+ immune cell-based patient selection for chemotherapy-free radioimmunotherapy in locally advanced head and neck cancer. *Journal for Immunotherapy of Cancer*. 2022; 10: e003747.
- [83] Sun XS, Tao Y, Le Tourneau C, Pointreau Y, Sire C, Kaminisky MC, *et al*. Debio 1143 and high-dose cisplatin chemoradiotherapy in high-risk locoregionally advanced squamous cell carcinoma of the head and neck: a double-blind, multicentre, randomised, phase 2 study. *The Lancet. Oncology*. 2020; 21: 1173–1187.
- [84] Ma SR, Deng WW, Liu JF, Mao L, Yu GT, Bu LL, *et al*. Blockade of adenosine A2A receptor enhances CD8+ T cells response and decreases regulatory T cells in head and neck squamous cell carcinoma. *Molecular Cancer*. 2017; 16: 99.
- [85] Chi H, Xie X, Yan Y, Peng G, Strohmmer DF, Lai G, *et al*. Natural killer cell-related prognosis signature characterizes immune landscape and predicts prognosis of HNSCC. *Frontiers in Immunology*. 2022; 13: 1018685.
- [86] Bisheskar SK, De Ruiter EJ, Devriese LA, Willems SM. The prognostic role of NK cells and their ligands in squamous cell carcinoma of the head and neck: a systematic review and meta-analysis. *Oncoimmunology*. 2020; 9: 1747345.
- [87] Johnson DE, Burtneess B, Leemans CR, Lui VWY, Bauman JE, Grandis JR. Head and neck squamous cell carcinoma. *Nature Reviews. Disease Primers*. 2020; 6: 92.
- [88] Wang C, Li Y, Jia L, Kim JK, Li J, Deng P, *et al*. CD276 expression enables squamous cell carcinoma stem cells to evade immune surveillance. *Cell Stem Cell*. 2021; 28: 1597–1613.e7.
- [89] Galon J, Bruni D. Approaches to treat immune hot, altered and cold tumours with combination immunotherapies. *Nature Reviews. Drug Discovery*. 2019; 18: 197–218.
- [90] Sacco AG, Chen R, Worden FP, Wong DJL, Adkins D, Swiecicki P, *et al*. Pembrolizumab plus cetuximab in patients with recurrent or metastatic head and neck squamous cell carcinoma: an open-label, multi-arm, non-randomised, multicentre, phase 2 trial. *The Lancet. Oncology*. 2021; 22: 883–892.
- [91] Oliva M, Spreafico A, Taberna M, Alemany L, Coburn B, Mesia R, *et al*. Immune biomarkers of response to immune-checkpoint inhibitors in head and neck squamous cell carcinoma. *Annals of Oncology: Official Journal of the European Society for Medical Oncology*. 2019; 30: 57–67.
- [92] . Epacadostat Shows Value in Two SCCHN Trials. *Cancer Discovery*. 2017; 7: OF2.
- [93] Gong X, Chi H, Xia Z, Yang G, Tian G. Advances in HPV-associated tumor management: Therapeutic strategies and emerging insights. *Journal of Medical Virology*. 2023; 95:

- e28950.
- [94] Gong X, Xiong J, Gong Y, Zhang J, Zhang J, Yang G, *et al.* Deciphering the role of HPV-mediated metabolic regulation in shaping the tumor microenvironment and its implications for immunotherapy in HNSCC. *Frontiers in Immunology*. 2023; 14: 1275270.
- [95] Xiong J, Chi H, Yang G, Zhao S, Zhang J, Tran LJ, *et al.* Revolutionizing anti-tumor therapy: unleashing the potential of B cell-derived exosomes. *Frontiers in Immunology*. 2023; 14: 1188760.
- [96] Song B, Wu P, Liang Z, Wang J, Zheng Y, Wang Y, *et al.* A Novel Necroptosis-Related Gene Signature in Skin Cutaneous Melanoma Prognosis and Tumor Microenvironment. *Frontiers in Genetics*. 2022; 13: 917007.
- [97] Gao W, Zhang ZW, Wang HY, Li XD, Peng WT, Guan HY, *et al.* TMED2/9/10 Serve as Biomarkers for Poor Prognosis in Head and Neck Squamous Carcinoma. *Frontiers in Genetics*. 2022; 13: 895281.
- [98] Affo S, Yu LX, Schwabe RF. The Role of Cancer-Associated Fibroblasts and Fibrosis in Liver Cancer. *Annual Review of Pathology*. 2017; 12: 153–186.
- [99] Biffi G, Tuveson DA. Diversity and Biology of Cancer-Associated Fibroblasts. *Physiological Reviews*. 2021; 101: 147–176.